

UNIVERSITY OF CALGARY

Characterization and Developmental Functions of the *C. elegans ing-3* Gene  
Product

by

Jingjing Luo

A THESIS

SUBMITTED TO THE FACULTY OF GRADUATE STUDIES  
IN PARTIAL FULFILMENT OF THE REQUIREMENTS FOR THE  
DEGREE OF MASTER OF SCIENCE

DEPARTMENT OF BIOCHEMISTRY AND MOLECULAR BIOLOGY  
CALGARY, ALBERTA  
AUGUST, 2007

© Jingjing Luo 2007



## UNIVERSITY OF CALGARY

The author of this thesis has granted the University of Calgary a non-exclusive license to reproduce and distribute copies of this thesis to users of the University of Calgary Archives.

Copyright remains with the author.

Theses and dissertations available in the University of Calgary Institutional Repository are solely for the purpose of private study and research. They may not be copied or reproduced, except as permitted by copyright laws, without written authority of the copyright owner. Any commercial use or publication is strictly prohibited.

The original Partial Copyright License attesting to these terms and signed by the author of this thesis may be found in the original print version of the thesis, held by the University of Calgary Archives.

The thesis approval page signed by the examining committee may also be found in the original print version of the thesis held in the University of Calgary Archives.

Please contact the University of Calgary Archives for further information,

E-mail: [uarc@ucalgary.ca](mailto:uarc@ucalgary.ca)

Telephone: (403) 220-7271

Website: <http://www.ucalgary.ca/archives/>

## Abstract

The inhibitor of growth (ING) proteins are involved in many biological pathways including tumour growth, chromatin remodeling, DNA damage-initiated stress signalling, and apoptosis (reviewed by Russell et al. 2006). ING proteins interact with core histones and associate with histone deacetylation/acetylation and contribute to epigenetic regulation. Here we identify and characterize a homolog of human ING3 in *C. elegans*, named *ing-3*. My project focused on determining the functions of *ing-3* and the relationship between *cep-1/p53* and *ing-3*. This work defined the subcellular localization of endogenous *C. elegans* ING-3 protein, investigated the two-promoter system of the *ing-3* gene, characterized the function of *ing-3* in regulating gamma radiation (IR)-induced germ cell apoptosis and body motility, and further determined that at least when promoting IR-induced germ cell apoptosis, *ing-3* and *cep-1/p53* act in the same functional pathway.

## **Acknowledgements**

I would like to thank my supervisor, Dr. Karl Riabowol, and my cosupervisor, Dr. Paul Mains for their guidance, encouragement and help. Thanks also to my committee members Dr. Jeb Gaudet and Dr. Randy Johnston for their great suggestions and advice, and to Dr. Peter Vize for spending precious time to serve as my external examiner.

Thanks to Dr. Jim McGhee and Dr. Dave Hansen for tons of counseling and help in my experiments. Thanks also to past and present members of the Riabowol, Mains and McGhee labs for their generous help and advice on my project, and to all members of the worm group for very informative discussion on every Monday morning.

Thanks to Chenggang Lu, Xiaolan Feng, Wei Gong, Cheryl Han, Jie Yan, Lindsay MacDonald and Keiko Suzuki for sharing their techniques and reagents with me. Thanks to my friends Lin Tang, Lin Ma and Dong Hu for their encouragement. Finally, thanks to my Mom and Dad, for their understanding, love and support all the time.

## Table of Contents

Approval Page.....	ii
Abstract.....	iii
Acknowledgements.....	iv
Table of Contents.....	v
List of Tables .....	vi
List of Symbols, Abbreviations and Nomenclature.....	viii
 CHAPTER I: INTRODUCTION.....	 1
 CHAPTER II: MATERIALS AND METHODS.....	 16
 CHAPTER III: RESULTS.....	 26
 PART 1: IDENTIFICATION AND CHARACTERIZATION OF <i>C. ELEGANS</i> <i>ING-3</i> GENE.....	 27
<i>C. ELEGANS</i> HAS THREE <i>ING</i> GENES.....	27
<i>C. ELEGANS</i> <i>ING-3</i> GENE IS BOTH SL1 AND SL2 TRANS-SPLICED.....	27
DIFFERENT PROMOTERS DRIVE <i>ING-3</i> EXPRESSION IN DIFFERENT TISSUES.....	28
 PART 2: IDENTIFICATION AND CHARACTERIZATION OF <i>ING-3</i> PROTEIN.....	 38
SEQUENCE ANALYSIS OF <i>C. ELEGANS</i> <i>ING-3</i> PROTEIN.....	38
ENDOGENOUS <i>ING-3</i> PROTEINS CAN BE RECOGNIZED BY SPECIFIC ANTIBODIES.....	39
<i>ING-3</i> ANTIBODIES STAINS IN NUCLEUS AND OVERLAP DAPI STAINING .....	40
 PART 3: <i>ING-3</i> PROMOTES IR-INDUCED GERM CELL APOPTOSIS .....	 51
DEPLETION OF <i>ING-3</i> INCREASES IR-INDUCED EMBRYONIC DEATH RATE ..	51
DEPLETION OF <i>ING-3</i> INHIBITS IR-INDUCED GERM CELL APOPTOSIS .....	53
<i>ING-3</i> KNOCKOUT MUTANTS.....	55
 CHAPTER IV: DISCUSSION .....	 64

**List of Tables**

Table 1. Best BLASTP matches to human and yeast ING proteins in <i>C. elegans</i> .....	30
Table 2. ING genes and proteins in <i>C. elegans</i> .....	31
Table 3. Embryonic death rates of different strains after 120Gy of IR.....	58
Table 4. Number of germ cell corpse/gonad after 120Gy of IR.....	60

## List of Figures and Illustrations

Figure 1. Diagram of the known structural features of the human ING family of proteins.....	13
Figure 2. Diagram of an adult hermaphrodite gonad.....	15
Figure 3. Genomic environment of <i>C. elegans ing-3</i> gene.....	32
Figure 4. Diagram of the GFP-LacZ reporter driven by “operon promoter”.....	33
Figure 5. Operon promoter-driven GFP and LacZ expression.....	34
Figure 6. Diagram of the GFP-LacZ reporter driven by “internal promoter”.....	35
Figure 7. Internal promoter-driven GFP and LacZ expression.....	36
Figure 8. Structure of <i>ing-3</i> gene .....	37
Figure 9. Sequence and predicted domains of ING3 protein.....	41
Figure 10. Phylogeny tree of ING3.....	42
Figure 11. Alignment of the ING3 protein sequence.....	43
Figure 12. Specificity of mouse ING-3 antisera on western blot.....	45
Figure 13. Localization of endogenous ING-3 protein.....	46
Figure 14. ING-3 expression in embryos.....	47
Figure 15. Specificity of mouse ING-3 antisera in immunostaining.....	49
Figure 16. IR-induced embryonic death rate.....	57
Figure 17. IR-induced germ cell apoptosis.....	59
Figure 18. ING-3 mutants.....	61
Figure 19. Unc phenotype of <i>ing-3</i> mutant strains.....	63
Figure 20. Linear relationship between the natural logarithm of the embryonic death rate and the dosage of $\gamma$ -irradiation.....	74

## List of Symbols, Abbreviations and Nomenclature

Symbol	Definition
AO	acridine orange
APS	ammonium persulfate
cDNA	complimentary DNA
DAPI	4'-6-diamidino-2-phenylindole
DIC	differential interference contrast
DNA	deoxyribonucleic acid
g	gram
HAT	histone acetyltransferase
HDAC	histone deacetylase
ING1	Inhibitor of Growth 1
IR	ionizing irradiation
kb	kilobase
kDa	kilodalton
LB	Luria-Bertani bacterial medium
mg	Milligram
ml	milliliter
mM	millimolar
mRNA	messenger RNA
ng	nanogram
NLS	nuclear localization signal
PBS	phosphate buffered saline
PCNA	proliferating cell nuclear antigen
PCR	polymerase chain reaction
PIP	PCNA interacting protein
RNA	ribonucleic acid
RNAi	RNA interference
RT	room temperature
SDS	sodium dodecyl sulphate
SDS-PAGE	SDS polyacrylamide gel electrophoresis
SL1	spliced leader 1
TAE	Tris-acetate EDTA buffer
TEMED	N,N,N',N'-tetramethylethyldiamine
UV	ultraviolet
µg	Microgram
µL	microliter
µM	micromolar
°C	degree Celsius
X-Gal	5-bromo-4-chloro-3-indolyl-β-D-Galactopyranoside

# **CHAPTER I: INTRODUCTION**

## **The ING family of PHD proteins**

The founding member of the ING (Inhibitor of Growth) family, ING1, was identified as a growth inhibitor and candidate tumour suppressor in 1996 by using a PCR-mediated subtractive hybridization approach to enrich for genes expressed in normal human mammary epithelial cells, but not in several breast cancer cell lines (Garkavtsev et al. 1996). Since then, additional ING proteins have been identified in various species based upon sequence homology (Nagashima et al. 2001, Nagashima et al. 2003). ING proteins have been found to be involved in many biological pathways including apoptosis, DNA repair, cell cycle regulation, chromatin remodelling, regulation of gene expression, DNA damage-initiated stress signalling, oncogenesis, tumour growth and angiogenesis (reviewed by Feng et al. 2002; Russell et al. 2006). All ING family members have a highly conserved plant homeodomain (PHD), a form of zinc-finger (Cys4-His-Cys3) that is associated with chromatin remodelling (Feng et al. 2002). So far there are five ING members (ING1-5) found in all mammals, including humans (Figure 1). Phylogenetic analysis showed that ING3 (which will be the focus of this work) is on a distinct branch while ING1 and ING2 are related, as are ING4 and ING5 in the parsimony tree (He et al. 2005). The arthropod ING proteins have paralogs corresponding to these three subgroups and may share some general features with their vertebrate counterparts (He et al. 2005). These sequence and structural groupings based on phylogeny appear to be conserved at the level of proposed cellular activity (Doyon et al. 2006). I will now discuss the many functions and the underlying mechanisms proposed for the ING family members.

### **Localization of ING proteins**

ING proteins are often found localized in the nucleus. Mislocalization or reduced nuclear localization of ING proteins is found in human cancers, suggesting that the nuclear localization may be related to the functions of ING proteins in tumorigenesis (Feng et al. 2002, Nouman et al. 2003, Vieyra et al. 2003, Lu et al. 2006).

Phosphorylation can regulate the localization and activity of ING proteins. The interaction between p33ING1b (one of the major splicing isoforms of ING1, Figure 1) and 14-3-3 was dependent on the phosphorylation status of p33ING1b and this interaction leads to the retention of p33ING1b protein in the cytoplasm and so affects the activity of p33ING1b (Gong et al. 2006). The localization of ING proteins is also mediated by stress signalling. Following ectopic overexpression or DNA damage, p33ING1b localized to nucleoli and this translocation appeared to promote apoptosis (Scott et al. 2001). Previous studies found that in the nucleus, ING proteins are involved in chromatin remodeling (described below).

### **ING proteins and chromatin modification**

ING proteins are involved in many biological functions and pathways. So far, how ING proteins coordinate so many functions is still unknown. However, we suspect that their multiple functionality might largely be brought about by the action of downstream effector genes mediated by ING proteins through chromatin modification.

The five ING subfamilies are all associated with HAT (histone acetyltransferase) or HDAC (histone deacetylase) complexes in mammalian cells (Doyon et al. 2006). A splicing isoform of ING1, p47ING1a (Figure 1), interacts with HDAC1 and inhibits

histone acetylation (Vieyra et al. 2002). Another splicing isoform of ING1, p33ING1b, associates with both HAT and sin3 HDAC (Kuzmichev et al. 2002; Vieyra et al. 2002). Similar to ING1, ING2 is a component of an HDAC complex. ING4 associates with the HBO1 HAT while ING5 interacts with two distinct complexes containing HBO1 HAT or MOZ/MORF HATs (Doyon et al. 2006). These HATs and HDACs change chromatin conformation by deacetylating or acetylating core histone proteins and inducing either gene silencing or transcription. This feature is well conserved in lower organisms. In *Dictyostelium*, the depletion of the ING family protein DNG1 (the *Dictyostelium* homologue of human ING1 protein) led to altered histone modification (Mayanagi et al. 2005). Three yeast ING proteins Yng1, Yng2 and Pho23 regulate chromatin configuration differently by associating with distinct HAT or HDAC complexes (Loewith et al. 2000). Furthermore, the yeast NuA4 subcomplex counterparts in humans, Tip60, EPC1 and ING3, can form a recombinant complex efficiently to reconstitute HAT activity *in vitro* (Doyon et al. 2004).

ING proteins have also provided a link between histone acetylation and methylation since the PHD region of the INGs is targeted to methylated histone H3, with the degree of methylation determining binding affinity (Pena et al. 2006; Shi et al. 2006). Therefore, by epigenetic modification of chromatin conformation, ING proteins can affect the transcription of downstream genes and further mediate more cellular functions.

### **ING proteins and stress-induced apoptosis**

ING proteins have been found to be involved in promoting apoptosis in response to DNA damage or when ING proteins are overexpressed. DNA damage induced by

etoposide and neocarzinostatin promoted ING2 expression (Nagashima et al. 2001), suggesting that the overexpression of ING proteins might mediate stress signal transduction.

p33ING1b synergizes with tumour necrosis factor alpha (TNF-alpha) in promoting apoptosis and induces expression of HSP70 in response to TNF-alpha (Feng et al. 2006). This was correlated with reduced NF-kappaB-dependent transcription, providing a link between p33ING1b induced apoptosis and the stress-regulated NF-kappaB survival pathway (Feng et al. 2006). In addition, apoptosis initiated by growth-factor deprivation occurred concurrently with the expression of the ING1 gene (Helbing et al. 1997, Ha et al. 2002). In several immortalized cell lines, overexpression of p33ING1b promoted variable levels of apoptosis (Helbing et al. 1997, Shinoura et al. 1999; Vieyra et al. 2002). Following UV irradiation, p33ING1b contributed to cell cycle arrest and either promoted DNA repair or induced apoptosis by binding proliferating cell nuclear antigen (PCNA), thus regulating a switch from DNA replication to DNA repair/apoptosis (Scott et al. 2001). In addition to ING1, ING2 or ING3 overexpression induced apoptosis (Nagashima et al. 2001, Nagashima et al. 2003). In response to cellular stress, ING2 was suggested to function as a nuclear receptor of phosphatidylinositol-5-phosphate (PtdIns5P) through the PHD domain, regulating DNA damage-initiated stress signalling to promote apoptosis (Gozani et al. 2003). In melanoma cells, overexpression of ING3 leads to caspase-8 dependent apoptosis after UV irradiation (Wang and Li 2006).

ING proteins in other model organisms indicate conservation of the role in stress-induced apoptosis. In mice, mING1 (mouse ING1) enhances serum starvation-induced cell death (Ha et al. 2002). Consistent with a function in apoptosis, disruption of ING1b

or of all ING1 splicing isoforms leads to increased sensitivity to gamma irradiation in mice (Coles et al. 2007, Kichina et al. 2006). In *Xenopus*, higher expression levels of xING2 (*Xenopus* ING2) were detected in several normal cell types undergoing apoptosis. Treatment of isolated organ cultures with thyroid hormone also induced the expression of ING proteins concomitantly with the induction of apoptosis (Wagner et al. 2001), indicating that the ING proteins are hormone sensitive transducers of apoptotic signals. Therefore, stress-induced apoptosis might be an evolutionally conserved function of ING proteins in other species, including *C. elegans*, and this will be a major question addressed in this thesis.

### **p53 and stress-induced apoptosis**

p53 is one of the most important tumour suppressor genes, with mutations of p53 found in many types of tumours (reviewed by Joerger and Fersht, 2007). When cells are subjected to stress signals such as DNA damage, hypoxia and oncogene activation, the ubiquitin-dependent degradation of the p53 protein is blocked and p53 is activated to induce apoptosis and/or cell cycle arrest (reviewed by Horn and Vousden, 2007). p53 regulates the apoptotic elimination of irreparably damaged cells through the transcriptional activation of its target genes, which is crucial to maintaining genome stability (reviewed by Fisher, 1994). Upon activation, p53 mediates apoptosis through a series of sequential events including Bax transactivation and translocation, the release of cytochrome c from mitochondria, caspase-9 activation, and the activation of caspase-3, caspase-6, and caspase-7 (Mihara et al., 2003, Chipuk et al. 2004, Danial and Korsmeyer 2004).

## **ING proteins and p53**

Both ING proteins and p53 are important regulators of stress-induced apoptosis and they have been suggested to synergize with each other. However, there is still controversy over the relationship between ING proteins and p53 in promoting apoptosis. Several mechanisms have been suggested.

In several immortalized cell lines, overexpression of p33ING1b promoted variable levels of apoptosis with p53 (Helbing et al. 1997; Shinoura et al. 1999; Vieyra et al. 2002; Zhu et al. 2005). Similarly, ING2 overexpression promoted a p53-dependent apoptosis, inhibited cell growth and induced G1 phase cell cycle arrest (Nagashima et al. 2001). ING2 enhanced the transactivation activity of p53 by increasing the acetylation of p53 (Nagashima et al. 2001). It was found that ING2 formed a complex with p53 and the histone acetyltransferase p300, assisting p300 to acetylate p53, and promoted p53-dependent replicative senescence (Pendeux et al. 2005). Ectopic ING3 transactivated p53 downstream genes and induced p53-dependent apoptosis (Nagashima et al. 2003). Both ING4 and ING5 overexpression could activate the p53 downstream gene p21/waf1 and lead to p53-dependent apoptosis (Shiseki et al. 2003). Similar to ING2, ING4 and ING5 enhanced p53 acetylation, and physically interacted with p53 and p300 *in vivo* (Shiseki et al. 2003). In yeast, Yng2 activated p21 in a p53-dependent manner as a component of NuA4 HAT complex (Loewith et al. 2000, Nourani et al. 2001).

However, ING proteins were also found to induce apoptosis in a p53 independent manner. p33ING1b and mING1 induced apoptosis in cell lines that lack p53 function (Tsang et al. 2003, Coles et al. 2007). In melanoma cells, ING3 induced Fas/caspase-8 dependent but p53-independent apoptosis following UV irradiation (Wang and Li, 2006).

We decided to study *C. elegans* ING proteins to clarify the functional relationship between ING proteins and p53, since *C. elegans* has proven to be a very useful genetic and developmental model organism for the study of gene regulation and function ([www.wormbook.org](http://www.wormbook.org)). Furthermore, many important cellular mechanisms, including the genetic pathway controlling apoptosis, have been well-characterized in *C. elegans* (Ellis and Horvitz 1986).

### **The *C. elegans* genetic system**

The small size, completely sequenced genome, fast life cycle and self-fertility of *C. elegans* make it a great model organism for genetic and developmental studies. Under the microscope, all 959 somatic cells of its transparent body are visible and all the lineages are traceable (Sulston and Horvitz 1977, Riddle et al. 1997). Furthermore, several molecular biological techniques for the manipulation of the genome are available to *C. elegans* research such as transgenesis, gene knockouts and RNA-mediated interference (RNAi) ([www.wormbook.org](http://www.wormbook.org)). These approaches are very useful in understanding genetic pathways and gene functions.

*C. elegans* shares cellular and molecular structures, regulatory pathways and complex developmental processes with more complex organisms. Although the nematode is small and simple, it still possesses many of the same tissues of higher organisms such as intestine, gonad and neurons. Many *C. elegans* genes have human homologs with similar functions (Riddle et al. 1997). Thus, the information learned from *C. elegans* may be applicable to higher organisms, such as humans.

### **Apoptosis in the *C. elegans* germline**

In *C. elegans*, the somatic cells have a fixed division program and tumours do not develop (Hengartner 1997). However, in the germ line, nuclei can continuously divide for indeterminate rounds and many undergo physiological programmed cell death. Following genotoxic stresses, the damaged germ cells will undergo checkpoint arrest and DNA-damage induced apoptosis, which makes it a perfect model for investigating gene function in apoptosis (Schedl 1997).

The *C. elegans* germline consists of two mirror-image U-shaped loops that empty into a common proximal vulva, through which eggs are laid. The distal germ line in each loop is syncytial until past the loop (Figure 2). In the adult gonad, germ cells undergo mitotic proliferation in the distal end, then progress through a transition zone and enter meiosis, preparing the oocyte for fertilization (Schedl 1997). The different stages can be readily distinguished by DAPI (4',6-diamidino-2-phenylindole) staining. The distal mitotic nuclei are uniform in size and have a brighter fluorescence on their circumference than in the centre (reviewed by Hubbard and Greenstein 2000, Hansen et al. 2004). The germ cells in the transition zone, which are progressing into the early phases of meiotic prophase, have a condensed and crescent-shaped morphology (Hansen et al. 2004). After going through the transition zone, the germ cells enter the pachytene stage and the chromosomes begin to individualize. Progression of nuclei into diplotene occurs in the loop of the gonad arm and the cells gradually become completely separated oocytes as they enter the proximal arm (Figure 2). At this stage, meiotic chromosomes exit diplotene and begin diakinesis with six highly condensed bivalents visible. In the end, the mature

oocytes will be fertilized by sperm stored in the spermatheca to become embryos (Schedl 1997, Hansen et al. 2004).

During this process, about half of the germ cells are estimated to be eliminated by apoptosis to maintain gonad homeostasis. Most of the germ cells apoptose during pachytene (Hengartner, 1997; Gumienny et al. 1999). Cell corpses are engulfed by the neighbouring gonadal sheath cells (Gumienny et al. 1999). Under Nomarski optics, the apoptotic germ cell is a flat, round, button-like disk (Sulston and Horvitz 1977, Hengartner 1997). When stained with acridine orange (AO), the apoptotic corpses can be easily detected under a microscope (Gumienny et al. 1999, Lettre et al. 2004).

Several distinct pathways have been found to regulate apoptosis in the germline (Gumienny et al. 1999, Gartner et al. 2000, Aballay et al. 2001). Execution of these cell death pathways depends on the core apoptotic machinery including *ced-3*, *ced-4* and *ced-9* (these are the homologs of the human genes Caspase-2, Apaf-1 and Bcl-2, respectively) (Gumienny et al. 1999, Gartner et al. 2000, Aballay et al. 2001, Salinas et al. 2006). Different stresses can activate different cell death pathways. Genotoxic agents and pathogen infection can promote germ cell apoptosis by activating an apoptotic pathway antagonized by *abl-1*, which involves the conserved apoptotic genes, *ced-3*, *ced-9* and *egl-1*; cell cycle checkpoint genes *clk-2*, *hus-1* and *mrt-2*; and the *C. elegans* p53 homolog, *cep-1* (Gartner et al. 2000, Deng et al. 2004). Using a different pathway oxidative, osmotic, heat shock and starvation stresses induce germ cell apoptosis independent of *cep-1* and *egl-1* (Salinas et al. 2006).

### **p53 in *C. elegans***

*cep-1* (*C. elegans* p53) is the *C. elegans* homolog of mammalian p53 (Derry et al. 2001, Schumacher et al. 2001). Although divergent from p53, CEP-1 possesses the DNA binding domain and includes the critical amino acids that are the most frequently mutated residues in human tumours and which are conserved in p53 members in other organisms (Derry et al. 2001). Also, CEP-1 is a transcription factor that can activate a reporter with human p53 binding sites (Derry et al. 2001). Similar to its mammalian counterpart, CEP-1 promotes germline apoptosis in response to genotoxic stress, suggesting that p53-mediated regulation of DNA damage-induced apoptosis is conserved during evolution (Derry et al. 2001, Schumacher et al. 2001). CEP-1 is ubiquitously expressed in embryos (Derry et al. 2001), while in the adult hermaphrodite germline, CEP-1 is abundant in mitotic germ cells in the distal arm (Schumacher et al. 2005). Germline CEP-1 then completely disappears from the transition zone and comes back in meiotic pachytene cells and remains during the diakinesis stage (Schumacher et al. 2005). Subcellularly, CEP-1 is localized to the nucleus and the protein level and localization do not change after IR (Schumacher et al. 2005). In worms, CEP-1 was found to regulate multiple stress responses in the soma, meiotic chromosome segregation and DNA damage-induced apoptosis in the germline (Derry et al. 2001, Schumacher et al. 2001).

### ***cep-1* and stress-induced apoptosis in *C. elegans***

CEP-1 mediates DNA damage-induced apoptosis, but not somatic apoptosis and physiological apoptosis in the *C. elegans* germline (Derry et al. 2001, Schumacher et al. 2001). Similar to the situation in mammalian cells, both UV and IR-induced apoptosis

and cell cycle arrest require CEP-1 (Derry et al. 2001, Schumacher B et al. 2001, Stergiou et al. 2007). Moreover, although *cep-1* did not affect germ cell apoptosis induced by oxidation or starvation, *cep-1* mutants exhibited hypersensitivity to hypoxia-induced lethality and decreased longevity in response to starvation, indicating that it may have other roles in the animal (Derry et al. 2001, Stergiou et al. 2007).

In mammals, ING proteins and p53 are important regulators of the genotoxic stress response and they have been found to synergize in promoting apoptosis. Furthermore, *cep-1/p53* induces apoptosis upon DNA damage through a pathway that is conserved from worm to human (Schumacher et al. 2001). Therefore *C. elegans* will be a good genetic model for studying the relationship between ING genes and p53.

### **Research hypotheses**

Work described in this research thesis was designed to test the following three hypotheses: first, since previous studies showed the evolutionary conservation of ING proteins in species from yeast to human beings, we proposed that in *C. elegans*, ING genes will regulate DNA damage-induced apoptosis as do other ING family members (He et al. 2005). Second, because mammalian ING genes localize in the nucleus and regulate chromatin configuration by histone acetylation or deacetylation, we proposed that the *C. elegans* ING genes may have analogous roles. Third, we proposed that the functional relationship between ING genes and p53 in promoting apoptosis is conserved in *C. elegans*. We predict that with the studies on *C. elegans* ING genes, we can be closer to understanding the mechanism of the regulation of apoptosis pathway that ING genes and p53 are involved in, which will provide valuable information for future medical research.

**Figure 1. Diagram of the known structural features of the human ING family of proteins**

There are five ING family proteins (ING1-ING5) in humans (He et al. 2005, Gong et al. 2006). The ING1 gene has four known alternative splicing variants. p47ING1a and p33ING1b are the two major splicing isoforms. Different conserved domains are indicated by different coloured boxes. All ING proteins possess the highly conserved plant homeodomain (PHD) region and a nuclear localization sequence (NLS) motif. Besides these common motifs, each ING protein or isoform also contains some other conserved regions. A leucine zipper-like (LZL) motif was found in ING2–ING5. p33ING1b has a proliferating cell nuclear antigen (PCNA)-interacting protein (PIP) domain while p47ING1a has a unique sequence in the N-terminus.

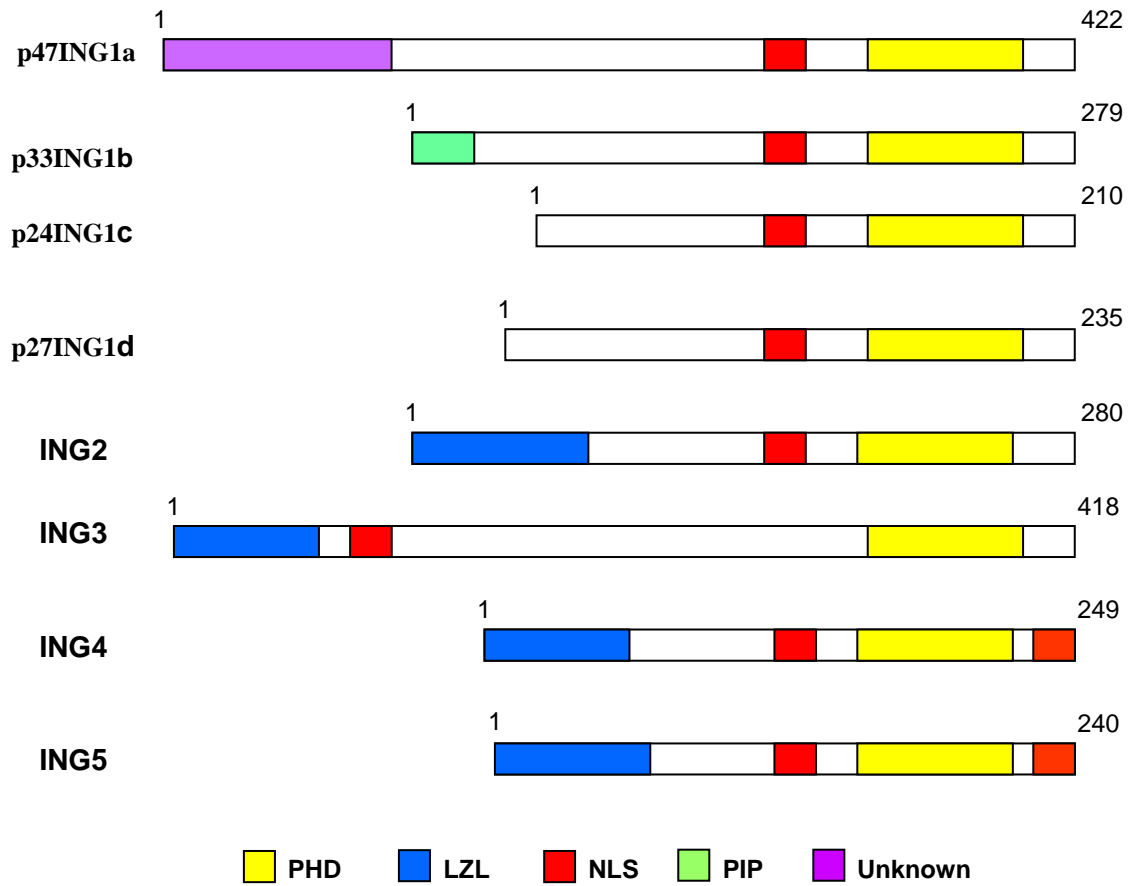
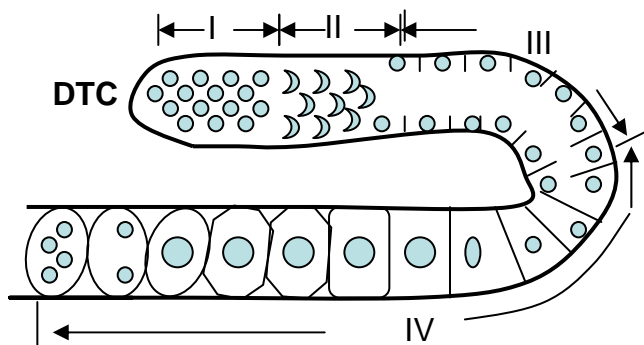


## Figure 2. Diagram of an adult hermaphrodite gonad

In the adult gonad, germ cells undergo mitotic proliferation in the distal end, starting from the somatic distal tip cell (DTC) (I), then progress through a transition zone (Schedl 1997, Hansen et al. 2004). The germ cells in the transition zone are progressing into the early phases of meiotic prophase and have a condensed and crescent-shaped morphology (II). After going through the transition zone, the germ cells enter the pachytene stage and the chromosomes begin to individualize (III). Progression of nuclei into diplotene occurs in the loop and the cells gradually become completely separated oocytes as they enter the proximal arm (IV). Finally, the mature oocytes will be fertilized and become the embryos (V).



## **CHAPTER II: MATERIALS AND METHODS**

## **I. General methods of *C. elegans***

### **i) *C. elegans* strains and maintenance**

All *C. elegans* strains used in this study were cultured and manipulated at 20°C with standard methods described by Brenner (Brenner 1974). The wild type strain is Bristol N2 and the mutant strains include *cep-1(gk138)*, *ing-3(ttTi5439)*, *ing-3(tm2530)*, *rrf-3(pk1426)*, *mcd-1(tm2169)* (Riddle and Albert, 1997). Additional information for each of these genes can be obtained from Wormbase (<http://www.wormbase.org>).

The nomenclature of *ing-3* followed the guidelines set by Horvitz (Horvitz et al., 1979). We named this gene according to its homology to human ING3. *ing-3(tm2530)* and *ing-3(ttTi5439)* were outcrossed three times prior to use in this analysis.

### **ii) Nomarski microscopy**

A 3% agarose pad was made on a glass slide and worms were mounted onto the pad in M9 buffer (Brenner 1974). 10 mM levamisole was applied to anaesthetize worms. After placing a coverslip on top, we sealed it with Vaseline to prevent dessication. Then the slides were viewed with an Axioplan microscope (Zeiss, Germany) for further observation. Images were taken and processed with AxioVision software (Zeiss, Germany) and Photoshop 7.0 (Adobe Systems, Inc., USA).

### **iii) Dissection**

About 150-200 young adult hermaphrodites (~1 day after moulting) for dissection were washed off the plates with PBS and rinsed once to remove bacteria. Levamisole was added into PBS to paralyze the worms in a glass dish. We used two 25-gauge needles like scissors to cut off the head and extrude at least one gonad arm in all animals. In some cases, the anterior part of the gut was also exposed. Excess liquid was then removed and

the dissected gonads fixed in formaldehyde/K<sub>2</sub>HPO<sub>4</sub> at room temperature (RT) for 20 min. After washing with PBST (described in Appendix) for once, the gonads were fixed in 100% methanol at -20°C for 5 min. Methanol was removed and gonads were washed in PBS twice before immunostaining.

#### **iv) Freeze-cracking method**

Embryos were fixed and permeabilized with the freeze-cracking method, as previously described (Miller and Shakes, 1995). Embryos were squeezed out of the bodies of the young adult hermaphrodites under a coverslip. After freezing on dry ice for 10 min, the coverslip was quickly removed with a razor blade and the embryos were fixed immediately in methanol and then acetone at -20°C. The embryo specimens were then rehydrated with decreasing concentrations of ethanol in PBST.

#### **v) Genomic DNA preparation**

97 µl worm lysis buffer (described in appendix) and 3 µl 20 mg/ml protease K were mixed together. 25 µl of this mixture and 10 young gravid adult worms were transferred to a PCR tube. This tube was then incubated at 65°C for 1 hr and 90°C for 15 min. The product, containing worm genomic DNA, was used in PCR.

## **II. Characterization of the *ing-3* gene**

### **i) Identification of homologs**

Homologs of *ing-3* gene were identified in *C. briggsae*, *Drosophila*, *Xenopus*, mouse and human with the BLAST program at the National Center for Biotechnology Information (NCBI) (<http://www.ncbi.nlm.nih.gov/BLAST/>). Multiple sequence alignments of ING3 were created with the CLUSTAL W program at the European

Bioinformatics Institute (<http://www.ebi.ac.uk/clustalw/>).

## ii) General molecular biology methods

PCR amplification and subcloning were carried out as described (Sambrook et al., 1989). Minipreps were performed following the Qiagen protocol (Qiagen, Germany).

A cDNA pool of mixed-stage worms was subjected to PCR amplification. A pair of specific primers (F1 and R1, list below) flanking the start and stop codons of *ing-3* were used to clone the coding region. The purified PCR product was gel purified and inserted into expression vector pQE30 (Qiagen, Germany) to produce ING-3 proteins with a 6×His tag at the N-terminus.

A polyT primer and nested gene specific primers (F2 and F3) were used to amplify the 3' end while splice leaders SL1, SL2, and nested gene specific primers (R2 and R3) were used to amplify the 5' end of *ing-3* (list below). The PCR products were gel purified and sequenced. DNA sequencing was performed by the DNALab Facility at the University of Calgary.

Oligonucleotide sequences are as follows:

F1: 5'-CATTGCATGCCTCTTCCTCGATGATTTTTT-3'

R1: 5'-CAGAAGCTTTTAGACTTCTCCCTCTTCGG-3'

SL1: 5'-GGTTTAATTACCCAAGTTTGAG-3'

SL2: 5'-GGTTTAACCCAGTTACTCAAG-3'

R2: 5'-ATTTGCGTTGAGCTAGCACG-3'

R3: 5'-CGGTCACCTCCTGAATTGTCG-3'

F2: 5'-AGAAGAGCTATGGAGATATG-3'

F3: 5'-ATCGGAGG ATGAGGAGGATG-3'

polyT: 5'-TTTTTTTTTTTTTTTTTTT-3'

### iii) Plasmid construction

The genomic sequences of the operon promoter (600 bp) and the *ing-3* specific internal promoter (880 bp) were obtained by PCR and subcloned into the promoterless GFP-LacZ reporter vector pPD96.04 (Andrew Fire, Stanford University, Stanford, CA) to create the transcriptional *ing-3* promoter-*gfp-LacZ* fusions. pPD96.04 contains a nuclear localization signal (NLS) and so the expressed GFP-LacZ fusion protein concentrates in the nucleus.

### iv) Transgenic worms

Transgenic strains were created by injecting 50 ng/μl of *ing-3* promoter-*gfp-LacZ* plasmid DNA with 50 ng/μl of pRF4 (*rol-6(su1006)*) (Mello et al. 1991) into the gonad of young hermaphrodites. F2 Offsprings with the Roller phenotype were taken as the transgenic lines and were confirmed by PCR. We generated more than six transgenic lines for both plasmids and saw no line-to line variation of GFP and LacZ expression patterns.

### v) β-gal staining

Worms in M9 buffer were placed onto slides and dried for 10 min. The worms were fixed and permeabilized with acetone for 30 min, and then incubated overnight with X-Gal to stain β-galactosidase (Zdinak et al. 1997).

### **III. Characterization of the expression of ING-3 protein**

#### **i) Antibody generation**

Both rabbit and mouse polyclonal antibodies against *C. elegans* ING-3 were generated by the Hybridoma Facility at the University of Calgary. Rabbits or mice were immunized with a KLH-conjugated synthetic peptide corresponding to the sequence CEMEADNSGVTEMIE (amino acids residues 108-122 located in the highly-conserved hydrophilic motif of the ING-3 protein). After subsequent boost injections, blood samples were collected every two weeks and the titers were tested by ELISA. The rabbit and the mouse were sacrificed for a final bleed when the antibody titer did not continue to increase. Serum was then separated from the whole blood. A series of test westerns were done to determine the yield and titer of the antisera.

#### **ii) Harvesting of *C. elegans* protein samples for SDS-PAGE gel**

100 post mounting young adult worms were transferred into an Eppendorf tube with 10  $\mu$ l PBS. 10  $\mu$ l 2xgel sample buffer was added and the sample was frozen at  $-80^{\circ}\text{C}$  for 5 min. Before loading on a SDS-PAGE gel, the samples were boiled for 5 min and centrifuged at 13,000g for 5 min.

#### **iii) Western blot analysis**

Western blots analysis was carried out following the standard procedures (Feng et al. 2006). Blots were blocked with 10% skim milk for 1 hr at room temperature (RT) then incubated with the mouse anti-ING-3 antiserum (diluted 2000 fold in 5% skim milk in PBST) overnight at  $4^{\circ}\text{C}$ . After washing three times for 10 min, the blot was incubated for 1 hr at RT with peroxidase conjugated goat anti-mouse IgG antibodies (diluted 4000 fold in 5% skim milk in PBST). Finally, the blot was washed three times and treated with

ECL chemiluminescence reagents. The level of actin was set as the internal loading control.

#### **iv) Immunofluorescence**

##### a) Dissected gonads

The dissected gonads were permeablized in PBST and blocked with 30% goat serum (in PBST) at RT for 4 hr. Then the gonads were incubated overnight at 4°C with the mouse anti-ING-3 antiserum, diluted 1:100 in 25% goat serum (in PBST). After washing the gonads three times for ten min with PBST to remove the unbound primary antibodies, gonads were incubated with Texas Red-conjugated goat anti-mouse IgG antibodies at RT for 4 hr, at 1:100 dilution in 25% goat serum (in PBST). Gonads were then washed for three times again and DAPI was added to stain nuclei. Gonads were then mounted on slides for microscopy.

##### b) Embryos

The difference between immunostaining of dissected gonads and embryos is in the concentration of the antibodies and the duration of incubation time. We blocked the embryo specimens with 25% goat serum at RT for 45 min, followed by incubation at 37°C for 1 hr with 1:100 diluted mouse anti-ING-3 antisera in 5% goat serum in PBST followed by 37°C for 1 hr with 1:100 diluted Texas Red-conjugated goat anti-mouse IgG antibodies in 5% goat serum in PBST. Other steps are the same as the gonad-staining procedures.

## IV. Functional studies

### i) RNAi interference (RNAi)

RNAi interference (RNAi) of *ing-3* was performed according to the standard procedure using the bacterial feeding method or the injection method (Timmons et al., 2001).

For RNAi by feeding, a 463 bp fragment of *ing-3* was cloned into the RNAi feeding vector L4440 between two T7 promoters in inverted orientation and the plasmid was transformed into *E. coli* HT115. Under the induction of IPTG, single-strand RNAs (ssRNA) from both directions are transcribed and will anneal with each other within the *E. coli* host to form dsRNA (Timmons and Fire, 1998). Wild-type worms fed *E. coli* HT115 containing the RNAi feeding vector L4440 were used as the control.

For RNAi injection, dsRNAs for microinjection were generated by *in vitro* transcription with the MEGAscript™ Purification Kit (Ambion) and *gfp* dsRNA was used as the control. Sense and antisense RNAs were transcribed separately and mixed together in equal amounts to anneal into dsRNA. 1 µg/µl dsRNA was injected into the gonads of the young adult hermaphrodites. Worms were transferred to a new plate 12 hr post-injection. Phenotypes were scored among the next 24 hr brood. In our experiments, *ing-3(RNAi)* by injection did not exhibit stronger phenotypes than *ing-3(RNAi)* by feeding.

### ii) Overexpression

To overexpress *ing-3* in *C. elegans*, a *hsp::ing-3* construct was generated and the plasmid DNA was injected into N2 worms. The ectopic expression of *C. elegans ing-3*

gene was under the control of the heatshock promoter of pPD49.83 (Andrew Fire, Stanford University, Stanford, CA) and was induced by treatment of 33°C for 1 hr.

## **V. Characterization of Phenotypes**

### **i) IR-induced embryonic lethality**

L4 stage animals were picked one day before irradiation. The next day, wild-type, mutant or RNAi young gravid adults were treated with different doses of  $\gamma$ -irradiation using a  $^{137}\text{Cs}$  source. Following irradiation, the worms were immediately transferred to new plates and the rate of embryonic death was scored for eggs laid during the first 0-8 h (irradiated between early embryogenesis and diakinesis stages) and 8-22 h (irradiated at pachytene stage) time periods (Takanami et al. 2000).

### **ii) IR-induced germ cell death**

L4 stage larvae were treated with 120 Gy  $\gamma$ -irradiation. Twenty-four hours later, the number of apoptotic germ cells per gonad arm was counted under Nomarski optics as described (Gumienny et al. 1999, Gartner et al. 2000). The result were confirmed by acridine orange (AO) staining. Worms were incubated with 500  $\mu\text{l}$  of 100 mM AO on plates for 1 hr then were transferred to clean plates and left in the dark for 1 hr. Worms were then mounted on slides and observed via fluorescence microscopy (Gartner et al. 2004, Lettre et al. 2004).

### **iii) Statistical analyses of germ cell apoptosis and embryonic death rate**

The statistics presented for each experiment includes the mean number of

apoptotic germ cells per gonad and mean embryonic death rate  $\pm$  standard deviation (SD).

**iv) Worm motility**

The videos recording worm movement were taken by a webcam (Logitech) attached onto a microscope and processed with the ImageStudio software (Logitech).

## **CHAPTER III: RESULTS**

## **PART 1: Identification and Characterization of *C. elegans* *ing-3* gene**

### ***C. elegans* has three ING genes**

Translated genomic sequences were searched using the BLAST program for proteins with the highest similarity to human ING proteins (Table 1). Three *C. elegans* genes, T06A10.4, Y51H1A.4 and C11G6.3, were found to encode ING proteins, corresponding to human ING1/2, ING3 and ING4/5 subgroups, respectively (Table 1, Table 2). Therefore, the genes T06A10.4, Y51H1A.4 and C11G6.3 were referred to as *C. elegans ing-1*, *ing-3* and *ing-4*, respectively in this thesis (although note that only *ing-3* is currently an official *C. elegans* gene name). Among the genes, ING3 and Y51H1A.4 have the most significant reciprocal scores (the lowest E values, Table 1, Table 2; a discussion of sequence conservation is described in Part 2). Thus, further studies focused on *ing-3* function.

### **The *C. elegans ing-3* gene is both SL1 and SL2 trans-spliced**

The *C. elegans ing-3* gene is the second gene in an operon on chromosome II that includes three other genes: mitochondrial dehydrogenase (Y51H1A.3), histone deacetylase *hda-6* and a C2H2 zinc finger protein *mcd-1* (Figure 3, [www.wormbase.org](http://www.wormbase.org)). In *C. elegans* 70% of mRNAs are trans-spliced to either of two 22 nucleotide spliced leaders, SL1 or SL2 (Blumenthal and Steward 1997). SL2 is spliced onto the downstream genes in operons while SL1 is used by the first gene in operons and for most genes that are not in operons. Some downstream genes in operons are also transcribed from both the operon promoter and an internal promoter, in which case they are spliced to both SL1 and SL2 (Blumenthal and Steward 1997).

To identify which splice leader is used by *ing-3*, splice leaders SL1, SL2, and nested gene-specific primers (materials and methods) were designed to amplify the 5' end of *ing-3* by PCR. Our sequenced PCR products showed that *ing-3* is both SL1 and SL2 trans-spliced, confirming the data in Wormbase ([www.wormbase.org](http://www.wormbase.org)). Furthermore, we noticed that the distance between *ing-3* and the upstream gene Y51H1A.3 was unusually long (more than 800bp) for an intergenic region in an operon. Therefore we suspected that *ing-3* might have two promoters and these two different promoters might result in different tissue-specific expression patterns of *ing-3*. GFP reporter genes driven by these two different promoter regions were used to test our speculation.

### **Different promoters drive *ing-3* expression in different tissues**

About 600 bp of the 5' genomic sequence of the first gene of this operon (Y51H1A.3), which extends to the neighbouring gene, has been used as the operon promoter while the genomic sequence of 880 bp between the start codon of *ing-3* and the stop codon of its upstream gene Y51H1A.3 has been used as the *ing-3* specific internal promoter. We obtained these two sequences by PCR and subcloned them into the vector pPD96.04 (Figure 4, Figure 6), which encodes a GFP/ $\beta$ -galactosidase fusion protein driven by the inserted promoter. The plasmid was injected into the gonads of wild-type worms to make transgenic lines.

Expression of *operon promoter::gfp/LacZ* was first detected during embryogenesis, at the stage of gastrulation (Figure 5). GFP expression was activated in pharynx, neurons, spermatheca and hypodermal cells, persisting through L1 larva to adulthood (Figure 5).

In contrast, the expression of the *internal promoter::gfp/LacZ* reporter began at a later time, at the comma stage (Figure 7). In larvae, GFP expression was detected in both the anterior and posterior intestine cells where it persisted through adulthood. Both GFP expression patterns directed by these two promoters were confirmed by the  $\beta$ -gal staining of the fused protein (Figure 5, Figure 7).

Based upon the different GFP expression patterns of the two promoters that we have observed, we suggest that *ing-3* might be transcribed both as part of an operon and independently, perhaps under different circumstances, and that these two patterns, together, reflect zygotic *ing-3* expression. Expression of both constructs was undetectable in the gonad of adult worms. However, since transgenes are almost inactive in the germline due to silencing (Kelly and Fire 1998), we cannot tell whether the *ing-3* gene is expressed in germ cells. It is also possible that the maternally-produced gene product is present in the early embryo before the onset of zygotic gene expression. Moreover, false positive GFP expression in the posterior gut and pharynx has been reported before. To address these issues, we generated antibodies to stain specifically the endogenous ING-3 protein, which will be described in Part 2.

**Table 1. Best BLASTP matches to human and yeast ING proteins in *C. elegans***

The sequences of different human and yeast ING proteins BLAST against the worm database, Y51H1A.4 (*C. elegans ing-3*) was always the best hit. Y51H1A.4 has the highest homology to human ING3 with the lowest E values ( $1.9e^{-33}$ ) of all BLAST.

		<b>Y51H1A.4</b>	<b>T06A10.4</b>	<b>C11G6.3</b>
<b>Human</b>	<b>p33ING1b</b>	$4.5e^{-15}$	$1.1e^{-11}$	$7.1e^{-09}$
	<b>p47ING1a</b>	$1.7e^{-13}$	$6.9e^{-11}$	$4.3e^{-08}$
	<b>ING2</b>	$2.3e^{-20}$	$8.0e^{-12}$	$1.9e^{-12}$
	<b>ING3</b>	<b><math>1.9e^{-33}</math></b>	$3.9e^{-12}$	$1.2e^{-07}$
	<b>ING4</b>	$2.5e^{-22}$	$3.4e^{-10}$	$6.4e^{-13}$
	<b>ING5</b>	$3.7e^{-22}$	$2.9e^{-13}$	$2.0e^{-10}$
<b>Yeast</b>	<b>YNG1</b>	$2.9e^{-15}$	$6.6e^{-12}$	$2.8e^{-08}$
	<b>YNG2</b>	$8.0e^{-21}$	$1.4e^{-12}$	$2.0e^{-05}$
	<b>PHO23</b>	$1.7e^{-12}$	$6.4e^{-09}$	$4.4e^{-05}$

**Table 2. ING genes and proteins in *C. elegans***

The predicted sequence of *C. elegans* ING proteins was used to BLAST against the human protein library, and identified human ING3 as the best hit to Y51H1A.4 with an E value of  $9e^{-17}$ . T06A10.4 is closest to p47ING1a (a major splicing isoform of ING1) while C11G6.3 is closest to ING4. ING3 and Y51H1A.4 have the most significant reciprocal scores.

<b>Gene Name</b>	<b>Sequence Name</b>	<b>BLASTP Best Hit</b>	<b>E Value</b>
<i>ing-3</i>	Y51H1A.4	ING3	$9e^{-17}$
<i>ing-1</i>	T06A10.4	p47ING1a	$3e^{-15}$
<i>ing-4</i>	C11G6.3	ING4	$7e^{-11}$

**Figure 3. Genomic environment of *C. elegans ing-3* gene**

The *C. elegans ing-3* gene is the second gene in an operon (Y51H1A) on chromosome II that includes three other genes: mitochondrial dehydrogenase (*Y51H1A.3*), histone deacetylase *hda-6* and a C2H2 zinc finger protein *mcd-1*.

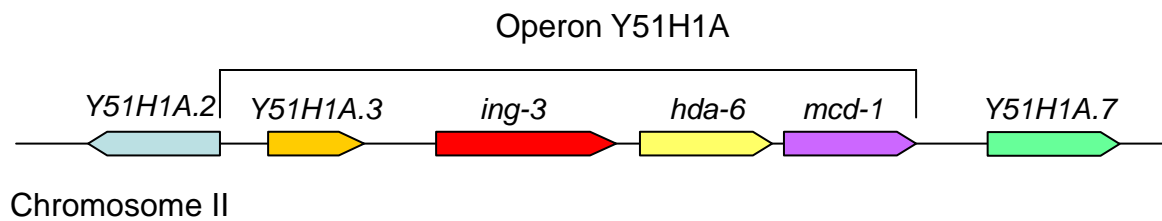


**Figure 4. Diagram of the GFP-LacZ reporter driven by operon promoter**

About 600 bp of the 5' genomic sequence of the first gene of this operon (Y51H1A.3) has been used as the operon promoter and subcloned into the vector pPD96.04, which encodes a GFP-LacZ fusion driven by the inserted operon promoter.

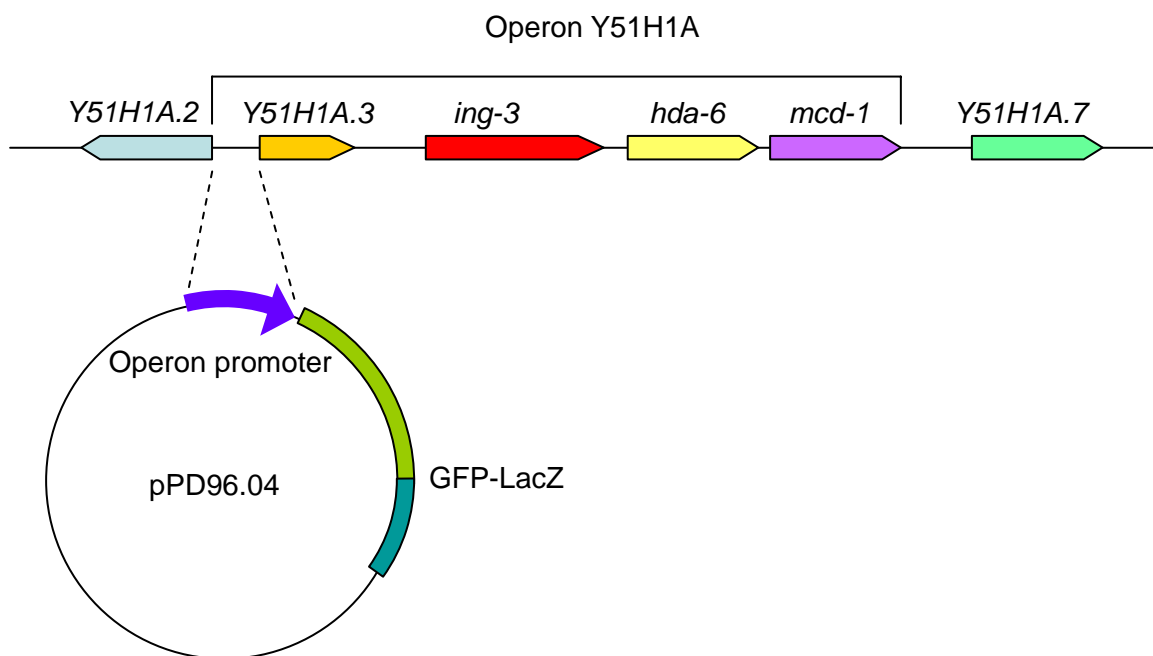


**Figure 5. Operon promoter-driven GFP and LacZ expression.**

The expression of *operon promoter::gfp/LacZ* was first detected during embryogenesis, at the stage of gastrulation. GFP expression was activated in pharynx, neurons, spermatheca and hypodermal cells, persisting through L1 larva to adulthood.  $\beta$ -gal staining of the fused protein confirmed the GFP expression pattern.

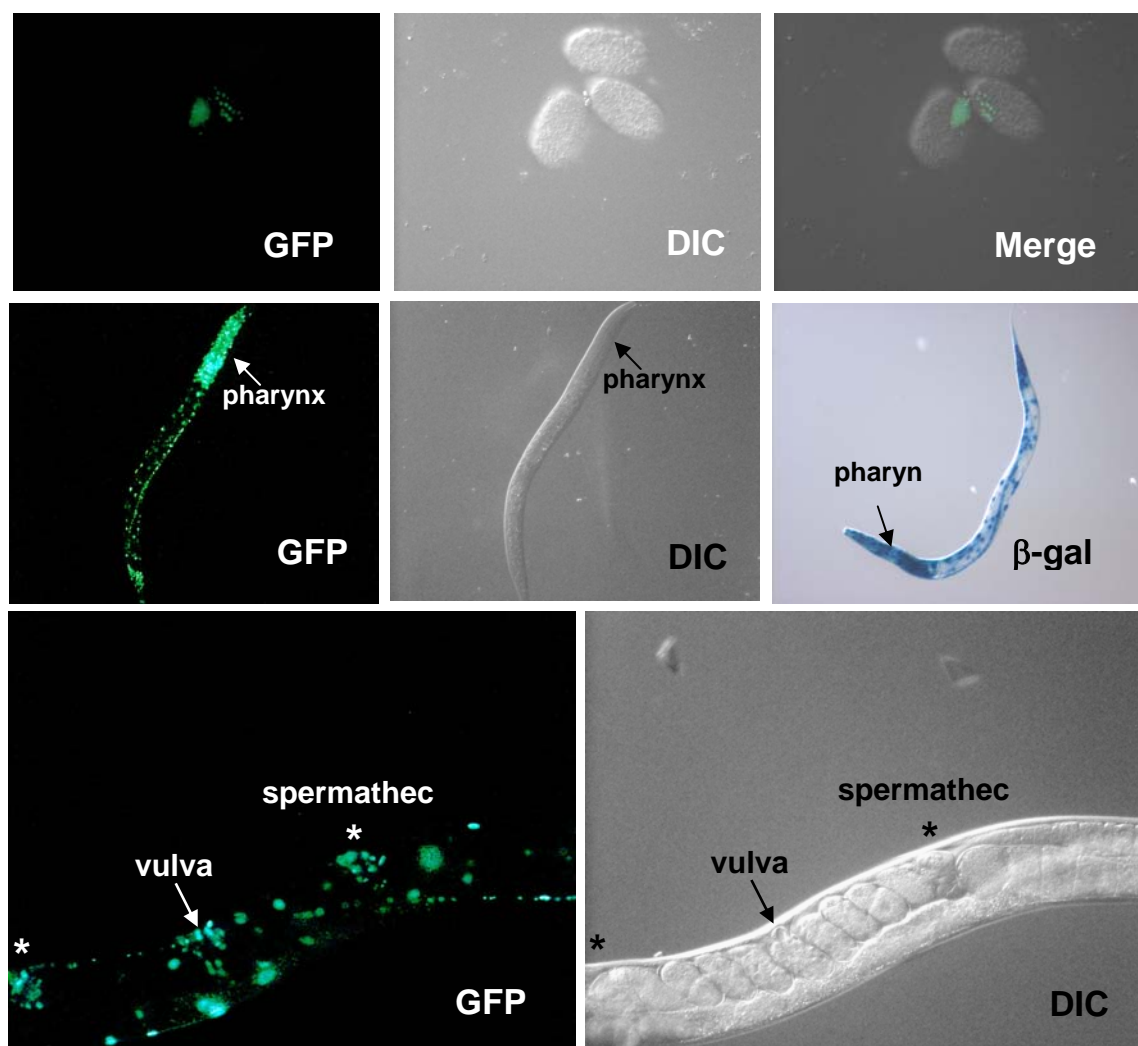


**Figure 6. Diagram of the GFP-LacZ reporter driven by internal promoter**

The genomic sequence of 880 bp between the start codon of *ing-3* and the stop codon of its upstream gene Y51H1A.3 has been used as the *ing-3* specific internal promoter and subcloned into the vector pPD96.04, which encodes a GFP-LacZ fusion driven by the inserted internal promoter.

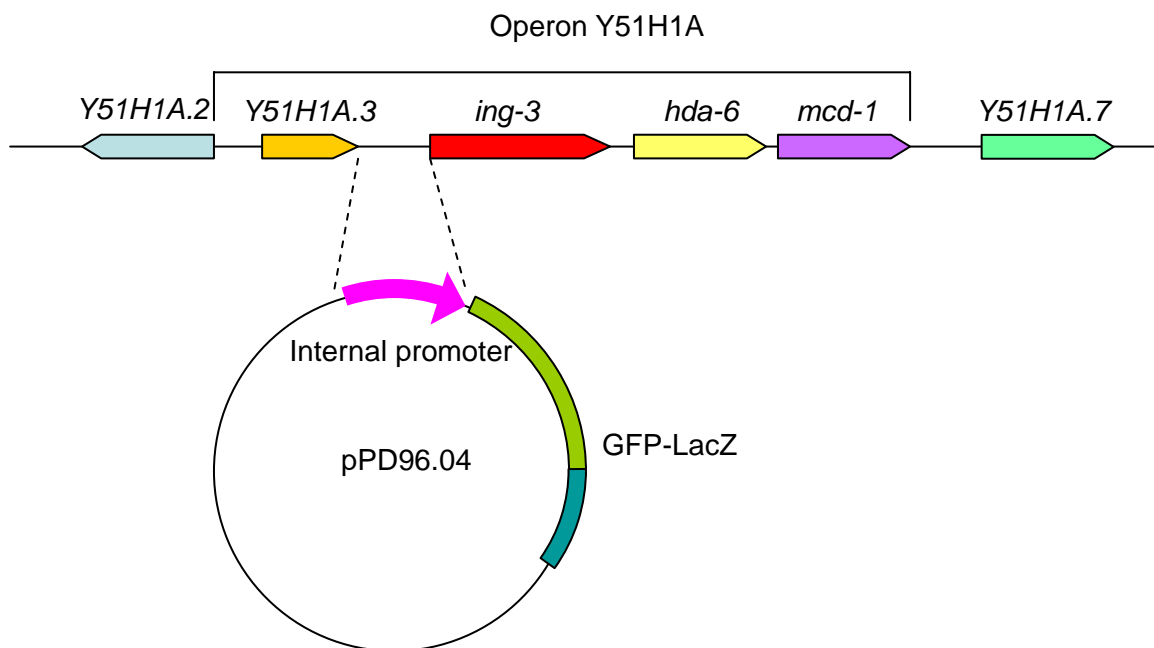


**Figure 7. Internal promoter-driven GFP and LacZ expression.**

The expression of the *internal promoter::gfp/LacZ* reporter began at the comma stage. In larvae, GFP expression was detected in both the anterior and posterior intestine cells where it persisted through adulthood.  $\beta$ -gal staining of the fused protein confirmed the GFP expression pattern.

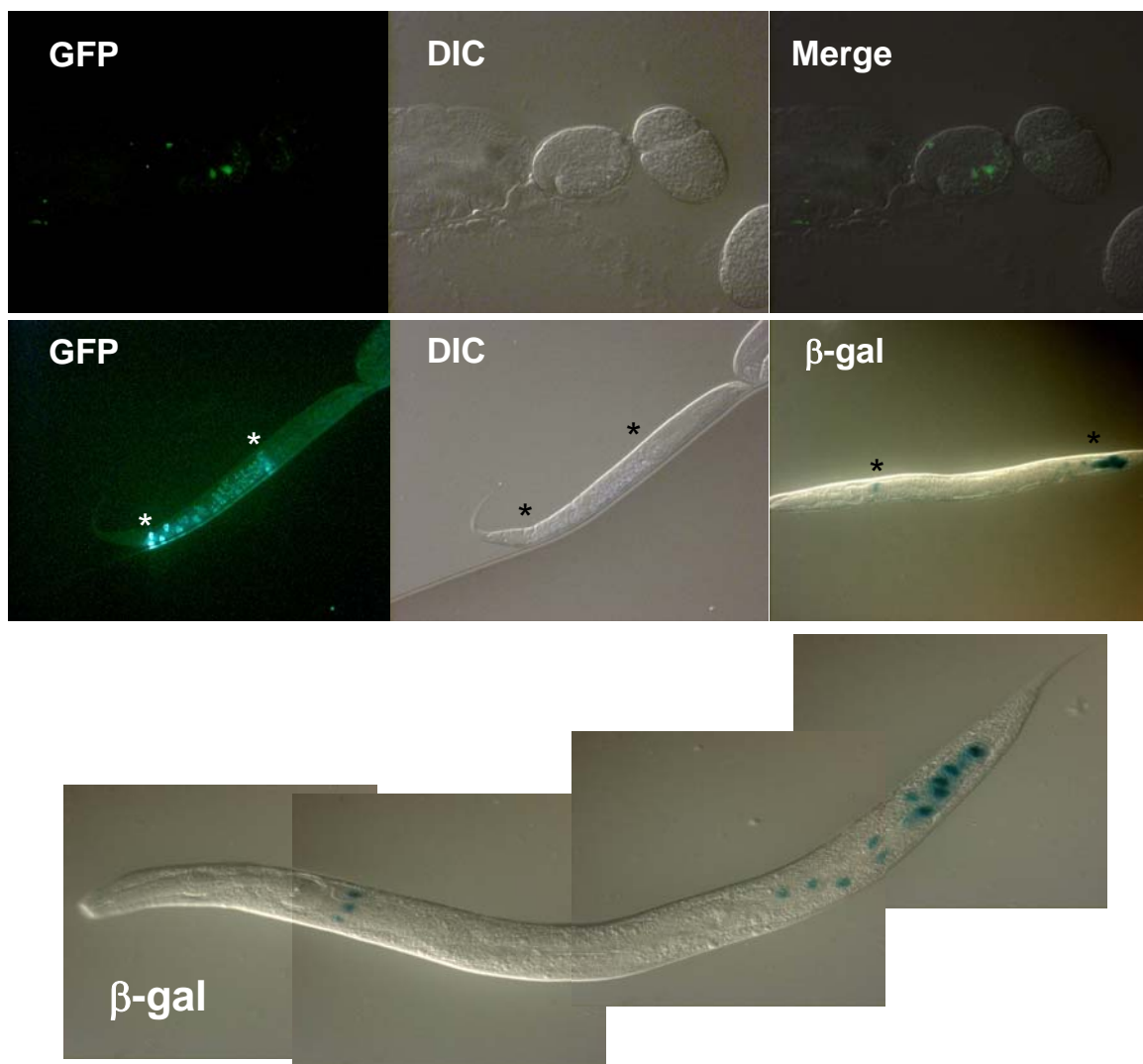
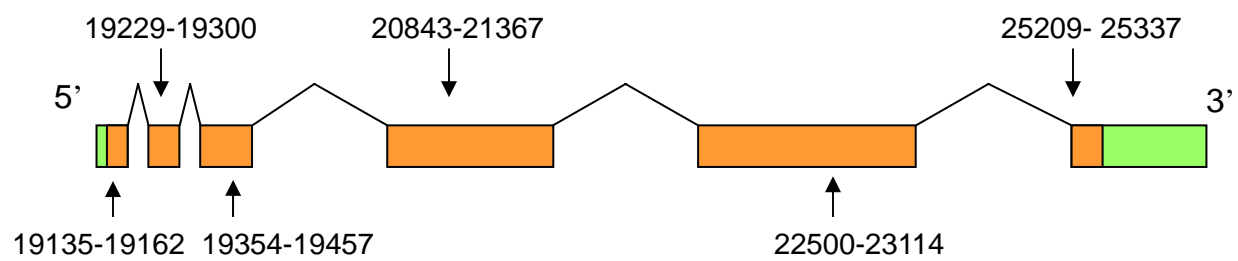


**Figure 8. The structure of *ing-3* gene**

The *ing-3* gene consists of 6 exons. The orange boxes represent exons while the green boxes indicate the 5' and 3' untranslated regions ([www.wormbase.org](http://www.wormbase.org)).



## **PART 2: Identification and Characterization of ING-3 protein**

### **Sequence analysis of the *C. elegans* ING-3 protein**

The full length coding region of *ing-3* was cloned from a cDNA pool of mixed-stage worms by PCR amplification with a pair of specific primers flanking the start and stop codons of *ing-3* (materials and methods). The sequencing results confirmed the predicted intron and exon boundaries of this gene that were outlined in Wormbase ([www.wormbase.org](http://www.wormbase.org)). The *ing-3* gene consists of 6 exons, encoding a 490 amino acid protein with a predicted molecular mass of 54.7 kDa and pI of 6.36 (Figure 8).

The predicted amino acid sequence of ING-3 indicates that it possesses a PHD zinc finger, an NLS sequence and a leucine-zipper-like (LZL) domain (Figure 9). The NLS sequence was found at amino acid 135-143, indicating that ING-3 might also localize to the nucleus as other ING proteins do. The PHD domain (C4HC3), conserved in all ING family members, is found at amino acids 430-474. Previous studies suggested that the PHD domain is involved in chromatin interactions (Pena et al. 2006). The leucine-zipper-like domain is located at the N-terminus at amino acids 1-36. This domain has been suggested to mediate protein–protein interactions (Wang et al. 2006).

The putative homologs of *C. elegans* ING-3 present in several organisms including human, mouse, yeast, *Drosophila* and *C. briggsae* are shown in Figure 10. When aligned with the Clustal W program (<http://www.ebi.ac.uk/clustalw/>), we found that in addition to the N-terminal leucine-zipper-like (LZL) domain and the C-terminal PHD domain, a hydrophilic motif (109 EMEADNSGVTEMIK 124) at amino acids 109-124, with unknown function, is highly conserved among all ING3 proteins from different species except yeast (Figure 11). The conservation of this motif suggested that it might be

important for the biological function of *ing-3*.

### **Endogenous ING-3 proteins can be recognized by specific antibodies**

Rabbit polyclonal antibodies targeting the highly conserved hydrophilic motif mentioned above were generated. The full length *ing-3* cDNA was cloned into pQE30 (QIAGEN) to produce a 6xHis Tag recombinant protein in *E. coli* M15 under induction by IPTG. The rabbit ING-3 antisera recognized this recombinant His-tagged ING-3 protein on western blots (not shown). However, there were many nonspecific bands when the endogenous ING-3 was detected on western blots (data not shown). Also, the rabbit antisera could not recognize endogenous ING-3 by immunostaining (data not shown). Therefore we generated mouse polyclonal antibodies targeting the same motif. The mouse antisera recognized endogenous ING-3 and presented a single 45 kD band on western blots, which indicated that we did not need to purify these antisera for immunostaining *in vivo*. Furthermore, the full length *ing-3* cDNA was cloned into pPD49.83 (Mello and Fire, 1995) and created a transgenic line carrying this plasmid to overexpress the wild-type ING-3 protein under the control of a heatshock inducible promoter *hsp16-41*. The *hsp::ing-3* strain increased levels of the 45 kD band on western blots after heat shock treatment, confirming its identity as ING-3 (data not shown). In addition, *ing-3(RNAi)* worms have a reduced level of the 45 kD band compared to wild-type animals on the western blot (Figure 12). Later we will show that *ing-3* mutants completely lack this band. These results suggest that the mouse polyclonal ING-3 antibodies specifically recognize ING-3 proteins. To examine the expression pattern of ING-3 at the cellular level, we stained the worms with these ING-3 antisera.

### **ING-3 antibodies stain in the nucleus and overlaps with DAPI staining**

Determination of the gene expression pattern will be helpful in determining the phenotypes of the RNAi animals and may give us hints as to possible biological functions. Immunofluorescence microscopy was used to stain the worms with the specific mouse polyclonal antibodies to determine the expression pattern of endogenous ING-3 protein.

ING-3 antibodies stained all adult tissues including the gonad, gut, neurons and many other cell types (Figure 13). ING-3 protein was detected in the germ cells of the gravid adult and during embryogenesis as early as one cell stage, suggesting its existence in the embryos before the onset of zygotic expression was due to a maternal contribution (Figure 13, Figure 14). In the gonad, ING-3 staining was weak in the mitotic proliferating germ cells but strong in the transition zone and the following pachytene stage, indicating a potential function in the germ line (Figure 13). At the subcellular level, ING-3 protein mainly localized in the nucleus, where it overlapped the DAPI pattern, which suggested that *ing-3* perhaps functions in chromatin regulation. *hsp::ing-3* and *ing-3(RNAi)* worms did not exhibit enhanced or decreased ING-3 immunostaining (data not shown), although changes were seen on Western blots. However, with peptide blocking or using the *ing-3* mutant strain (see Part 3), all of the described patterns disappeared, confirming specificity of the ING-3 antibodies in immunostaining (Figure 15).

Since *C. elegans* ING-3 is expressed in the germ line and embryos, we investigated the functions played by ING-3 in these tissues.

### Figure 9. Sequence and predicted domains of ING3 protein

ING-3 protein has a Leucine-Zipper-Like (LZL) domain in N-terminus, a NLS sequence in the middle and a PHD domain in C-terminus.

MLFLDDFLEMLDELPAELKERSDEIRRIDNEVESRLNRNREAINDFFERTGVNMPE  
**LZL**  
 EQRKERCKVLQEEFSTIRVLAQRKYLIAEKMQELLKKYKVHLEKEKTTFCEME  
 ADNSGVTEMIKRYTQHVESLLTARKERKRRHRVGGGGGGGGSSSRASTVASGP  
**NLS**  
 LLSKESKDKIQRILQEGVRLRMDLSDESAQSALSSAIPSPAPRGRPPKIAKDQLLS  
 SAAMVVASDDCLTPVPPTPTARRRSNTNALRGTVSIPSALSSMMNRGESTSRFSPN  
 PSERSWSNAGIDESSPTPTTSLMTPTFSSGPHIVVSPTTPVLQNSAFVVSESRHGR  
 TRKLTSRVQEMFKETLQRQRNHGNSIALQERMSAANLAAAQHAHAPTSSSPQS  
 PLPEIEGAAEDDDEEGPSYRIKRSHPMMPGSEDEEDEMHWCFNEKSYGDMV  
QCDNRHCTLRWFHYPCIGMVEPPTGKWYCPRCEVTMGI ALKLSEEDEV  
**PHD**

**Figure 10. Phylogeny tree of ING3**

The putative homologs of *C. elegans* ING-3 present in several organisms including human, mouse, yeast, *Drosophila* and *C. briggsae*.

Phylogram

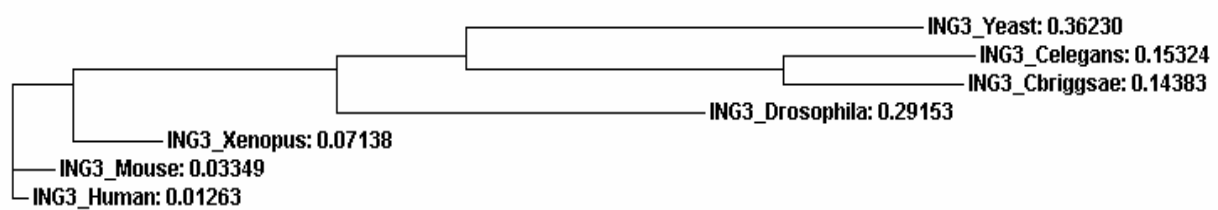


**Figure 11 . Alignment of the ING3 protein sequence.**

We aligned ING3 from various species including human, mouse, yeast, *Drosophila* and *C. briggsae*. Arrows indicate conserved motifs. We found that besides the N-terminal leucine-zipper-like (LZL) domain and the C-terminal PHD domain, a hydrophilic motif (109 EMEADNSGVTEMIK 124) with unknown function, is highly conserved among ING3 proteins in different species.

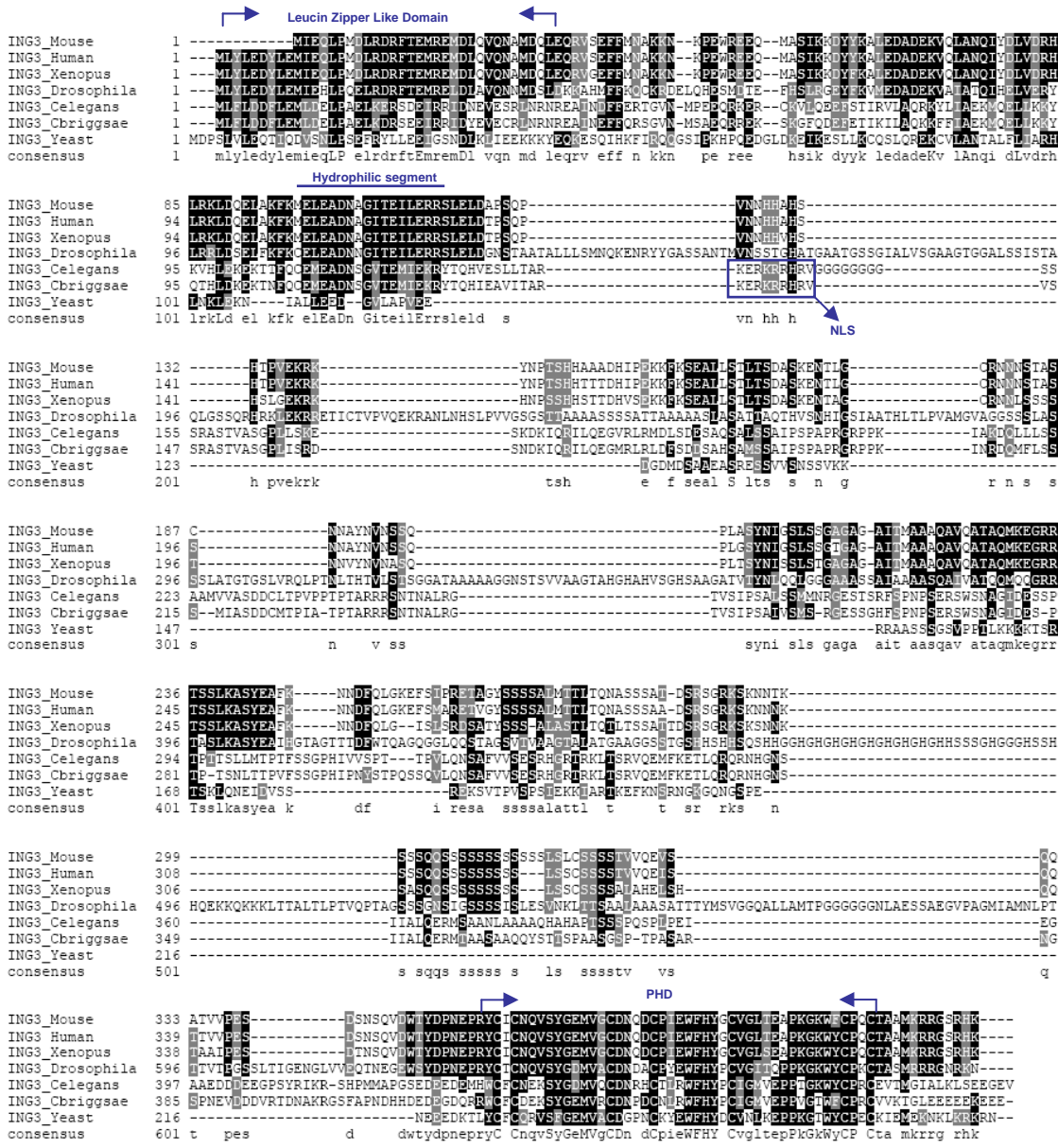


**Figure 12. The specificity of mouse ING-3 antisera in western blots**

The mouse polyclonal anti-ING-3 antisera recognized endogenous ING-3 protein and presented a single 45 kD band on western blots. *ing-3(RNAi)* worms have a reduced level of the ING-3 protein compared to the wild-type animals on the western blot.

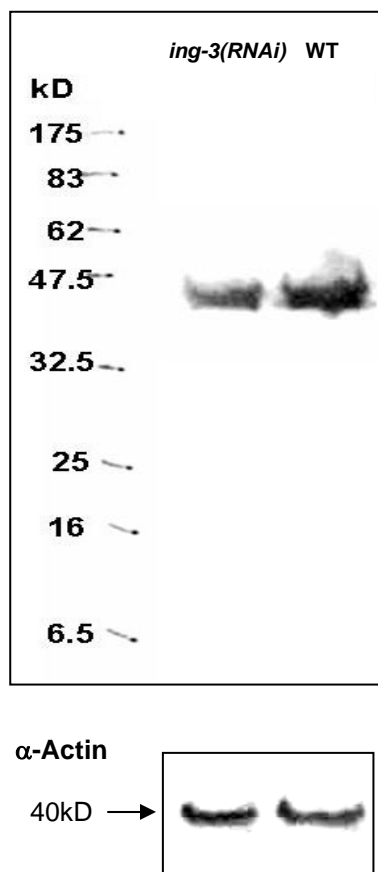


**Figure 13. The localization of endogenous ING-3 protein**

Mouse anti-ING-3 antibodies stained everywhere including the gonad, gut, neurons and many other tissues and cells. In the gonad, ING-3 staining is weak in the mitotic proliferating germ cells but strong in the transition zone and the following pachytene stage. In gut, ING-3 antibodies stained the anteriormost region. At the subcellular level, ING-3 protein mainly localized in the nucleus, where it overlapped the DAPI pattern.

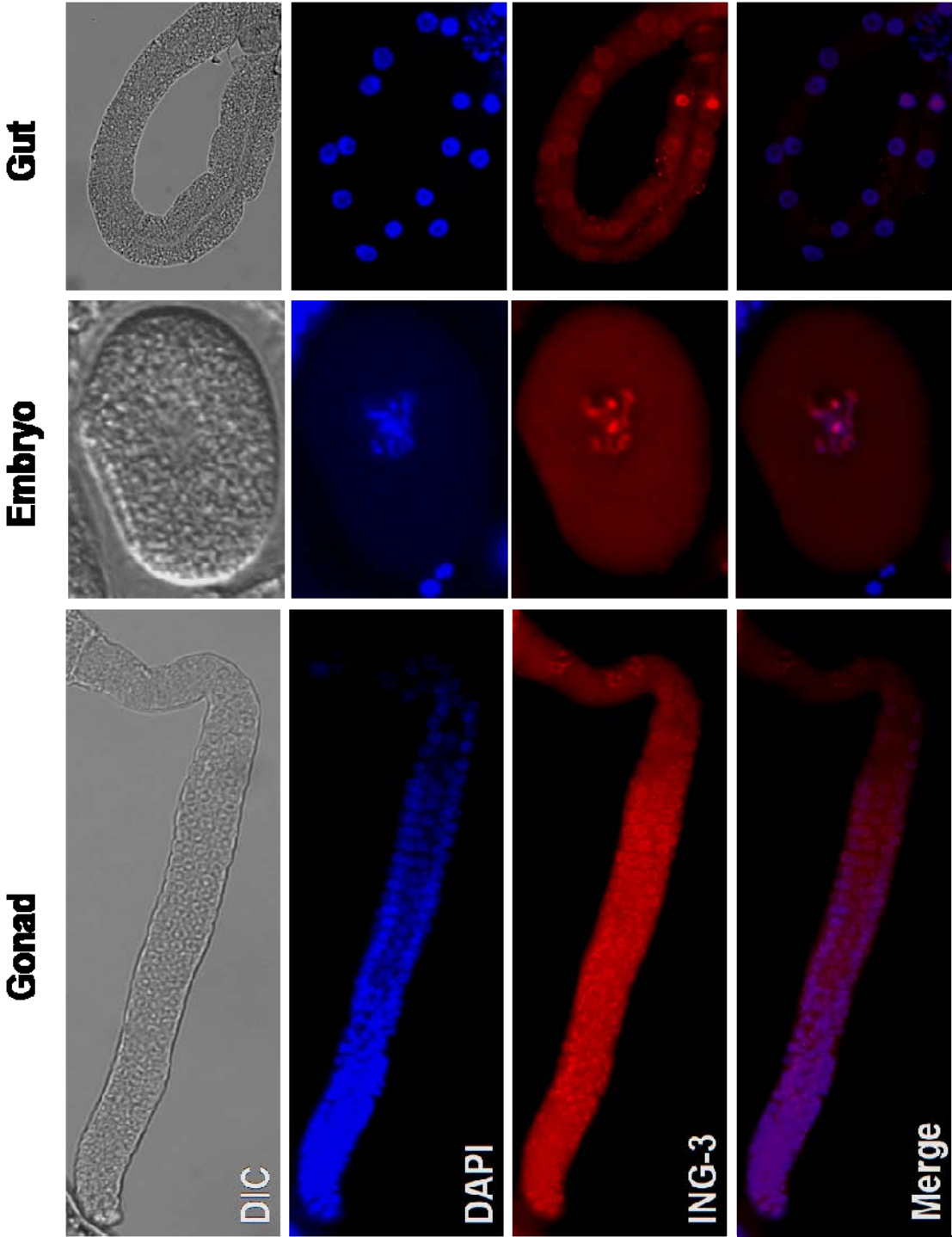


**Figure 14. ING-3 expression in embryos**

ING-3 protein was detected in the embryos at all stages, mainly localized in the nucleus and overlapping the DAPI pattern.

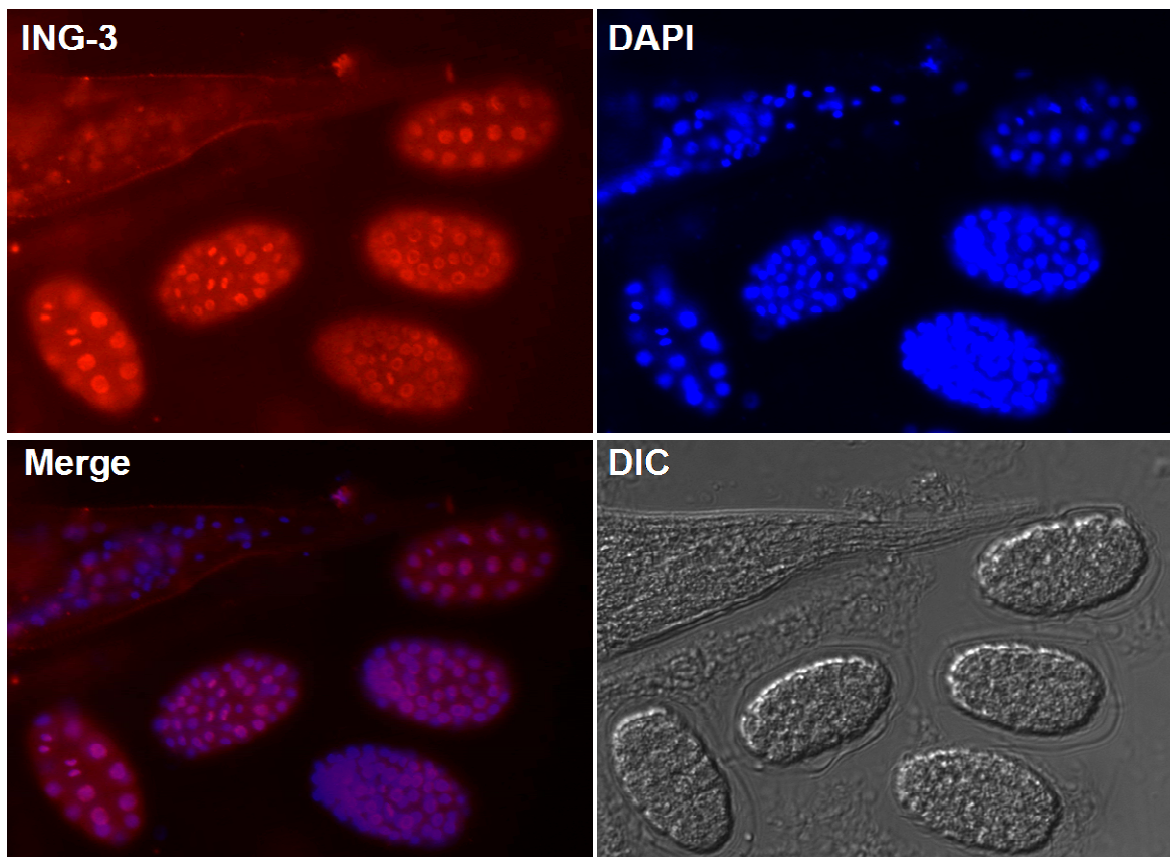
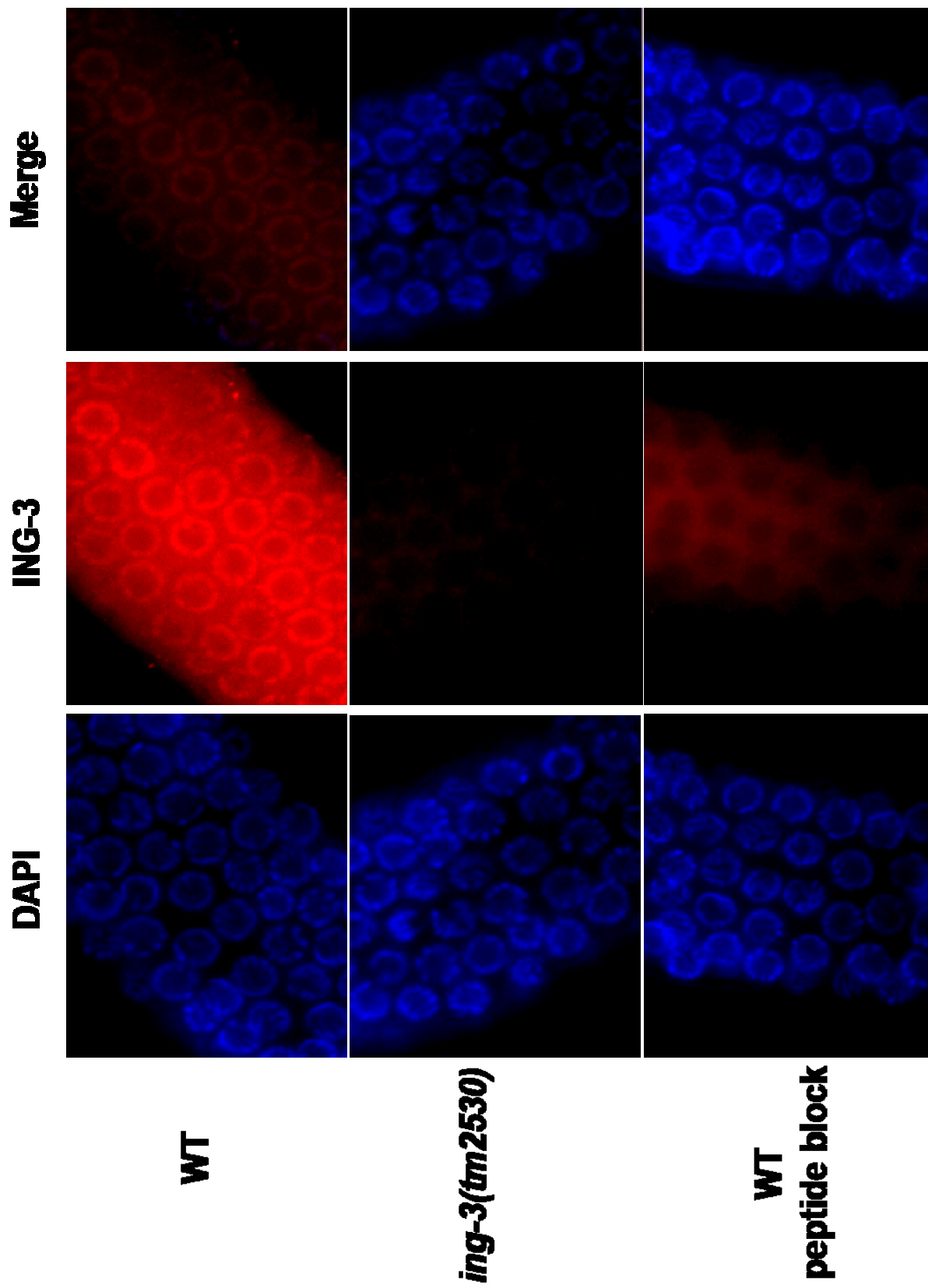


**Figure 15. The specificity of mouse ING-3 antisera in immunostaining**

In gonad, ING-3 antisera stained the nuclei of the germ cells and overlapped with the DAPI pattern. With peptide blocking or using the *ing-3* mutant strain, the nuclear staining disappeared.



### **PART 3: *ing-3* promotes IR-induced germ cell apoptosis**

#### **Depletion of *ing-3* increases IR-induced embryonic death rate**

Previous studies have showed that mammalian p33ING1b, ING2 and ING3 are all involved in DNA damage-induced stress response (Helbing et al. 1997, Ha et al. 2002, Shinoura et al. 1999, Scott et al. 2001, Nagashima et al. 2001, Vieyra et al. 2002, Gozani et al. 2003, Nagashima et al. 2003, Feng et al. 2006, Wang and Li 2006). Therefore we predicted that the *ing-3* gene might also function in response to DNA damage in worms.

At the beginning of this study, knockout mutants were not available, so RNAi was used to knock down expression of *ing-3*. RNAi has been demonstrated to be an efficient way to study gene function in *C. elegans* (Timmons and Fire, 1998). Genes in worms can be silenced by feeding, soaking or microinjection with double strand RNA (dsRNA). The phenotypes of *ing-3(RNAi)* worms were scored but no obvious phenotypes such as defects in movement, developmental timing, morphological changes or fertility were detected. Even in the genetic background of the RNAi enhancer mutant *rrf-3*, which should exhibit a better knockdown effect, no abnormalities were found. There was no increased embryonic death. However, as will now be described in detail, after gamma irradiation of hermaphrodites, the embryonic death rate of F1 progeny was elevated in the *ing-3* RNAi worms.

Young gravid adults of *ing-3(RNAi)*, *cep-1(ok138)*, and *ing-3(RNAi); cep-1(ok138)* were irradiated with different doses of UV or IR irradiation. RNAi was done by feeding and *ok138* is a null allele of the *C. elegans* p53 homolog *cep-1*. *hda-6(RNAi)*, *unc-86(RNAi)* and the wildtype were used as controls. Following irradiation, the worms were

immediately transferred to new RNAi feeding plates and the embryonic death rates of eggs laid during 0-8 and 8-22 hr post IR (which corresponds to irradiation at pachytene stage, Takanami et al. 2000) were scored (Table 3).

*cep-1* worms showed a higher IR-induced embryonic death rate in F1 progeny, consistent with the role of this gene in DNA damage-induced apoptosis (Derry et al. 2001, Schumacher et al. 2001). That is, if damaged embryos do not die, they go on to form inviable embryos. Interestingly, the enhanced IR-induced embryonic death rate of *ing-3(RNAi)* worms is comparable to that of *cep-1* worms (Figure 16), even though RNAi only reduced the ING3 protein level by 50% (this western blot has been repeated three times). The *ing-3(RNAi); cep-1* strain did not show a stronger effect than *ing-3(RNAi)* or *cep-1* by themselves, suggesting that these two genes function in the same pathway rather than in parallel pathways. At different doses of IR, *ing-3(RNAi)*, *cep-1* and *ing-3(RNAi); cep-1* strains all showed a higher embryonic death rate than the wild-type worms, but at 120 Gy, the difference is most prominent (nearly two-fold). The embryonic death rate of *unc-86(RNAi)* and the wild-type control were similar to each other, indicating the phenotype of *ing-3(RNAi)* is not a general artifact of RNAi.

It is intriguing that *ing-3* and *hda-6* histone deacetylase are in the same operon, because mammalian and yeast ING proteins are involved in chromatin acetylation/deacetylation. Although not generally the case, functionally related genes are sometimes found in the same *C. elegans* operon (Huang et al. 1994, Clark et al. 1994, Treinin et al. 1998). However, *hda-6(RNAi)* worms did not share the radiation sensitivity with *ing-3(RNAi)* (Table 3, Fig 16).

The embryonic death rates of the eggs laid during 0-8 hr post 120 Gy IR, which

corresponds to irradiation at embryogenesis and late pachytene, but did not show any differences between *ing-3(RNAi)* and wild-type worms (data not shown). Different dosages of UV irradiation were also used to treat the worms but no phenotype was found in *ing-3(RNAi)* worms (data not shown).

The cause of the enhanced embryonic death rate in *ing-3(RNAi)* was then explored. In multicellular animals, genotoxic stress induced DNA damage will lead to cell cycle arrest, DNA repair and/or apoptosis. The mammalian ING proteins are involved in regulating cell cycle arrest and apoptosis (reviewed by Feng et al. 2002). Since the *C. elegans* germ cells were irradiated at the non-dividing meiotic stage, defects in cell cycle arrest can be ruled out. This implies that the worms depleted of *ing-3* failed to undergo DNA repair or apoptosis in the germ line, and either of these cases could lead to production of zygotes with lethal DNA lesions. If *ing-3* is involved in apoptosis, the apoptotic germ cells in the gonads of the irradiated RNAi worms should be less than the control, and these damaged but non-apoptotic cells would produce inviable embryos. Therefore in the next experiments we compared the germ cell corpses in the *ing-3(RNAi)* worms and the wild-type control following IR.

### **Depletion of *ing-3* inhibits IR-induced germ cell apoptosis**

The germ lines of L4 hermaphrodite larvae are more sensitive to IR than are adults. Since the F1 embryonic death rate of RNAi and wild-type worms has the biggest difference at 120 Gy, we treated L4 stage larvae with this dose of IR. Twenty-four hrs later, the number of apoptotic germ cells per gonad arm was counted either in live animals under the Nomarski microscope (scoring the distinct morphology of apoptotic

cells) or by acridine orange staining of fixed animals (Figure 17). In *ing-3(RNAi)* worms, the number of apoptotic germ cells was nearly half that of the wild-type worms (Table 4). Without irradiation, *ing-3(RNAi)* worms and the control did not have any difference in the number of apoptotic germ cells and the embryonic death rate was similarly low in both cases, which suggested that *ing-3* does not function in physiological (i.e., the normal background) germ cell death. This result suggested that the increased embryonic lethality in the RNAi animals is because the damaged germ cells resist undergoing apoptosis and go on to form inviable zygotes.

The above results indicate that *ing-3* is involved in DNA damage-induced germ cell apoptosis. This may occur using the same pathway(s) as genes previously characterized for this function in *C. elegans*, such as *cep-1*. When *ing-3(RNAi)* was employed on the *cep-1(null)* mutant, the number of apoptotic cells was similar to *cep-1(null)* mutant or *ing-3(RNAi)* alone (Table 4), confirming the prediction that ING-3 and CEP-1/p53 are involved in the same pathway to promote apoptosis. However, the depletion of CEP-1 or ING-3 did not completely block germ cell apoptosis, suggesting that there is a CEP-1 and ING-3 independent pathway controlling IR-induced germ cell apoptosis.

Since loss-of-function in *C. elegans ing-3* by RNAi caused a hyposensitive DNA damage-induced apoptosis phenotype, we were interested in whether worms that overexpress *ing-3* are hypersensitive in DNA damage-induced apoptosis. Therefore, a gain-of-function study using heatshock induced ING-3 overexpression was performed. However, no change in the embryonic viability after IR (data not shown). Although increased expression was seen compared to wild type on the western blot (which would be the sum of germline and somatic expression), a stronger fluorescence signal in the

germ line was not detected (data not shown). This is likely because most transgenes are poorly expressed in the *C. elegans* germline (Kelly and Fire 1998).

### ***ing-3* knockout mutants**

Although RNAi is efficient and easy to perform, the knockdown is often transient, incomplete and variable. To overcome this problem, we requested *ing-3* mutations from the National Bioresource Project for the Nematode (Japan) (Gengyo-Ando and Mitani, 2000). In addition, the NEMAGENETAG Consortium (France) is isolating a large collection of random *Drosophila* Mos transposon insertions throughout the *C. elegans* genome (Granger et al., 2004). Near the end of this study, we received a homozygous deletion mutant strain *ing-3(tm2530)* and a heterozygous insertion mutant strain *ing-3(ttTi5439)* (Figure 18). The *ing-3(ttTi5439)* mutation was homozygosed and confirmed by PCR. Both of these *ing-3* mutant strains were found to be viable but possessed a weak kinker uncoordinated (Unc) phenotype even after outcrossing three times, so it is virtually certain that the Unc phenotype is due to the *ing-3* mutations. The *ing-3* knockout mutant worms bend with a sharper angle when moving and are slow in backing up after touching the head with a platinum wire (Figure 19).

In *ing-3(tm2530)*, the gene has a partial deletion in the 4<sup>th</sup> intron and the 5<sup>th</sup> exon, which might be translated into a 248 aa truncated protein with a predicted molecular mass of 27.9 kDa. In *ing-3(ttTi5439)* worms, the gene is interrupted by a Mos-1 insertion in the 4<sup>th</sup> exon and the first in-frame stop codon would result in a product of 17.2 kDa. Our mouse polyclonal antibodies recognize a motif encoded by the 4<sup>th</sup> exon, which is upstream of both mutations (Figure 18). Therefore the antibodies should be able to

recognize proteins encoded by the mutant genes. Western blots showed that the bands of 45 kD in both knockout strains are gone and none other appeared, demonstrating that ING-3 in these two strains are both completely depleted (Figure 18), suggesting they represent molecular nulls. The mutant proteins or transcripts are probably unstable and subjected to degradation.

*ing-3(null)* mutant worms were treated with 120 Gy IR. The phenotypes were slightly stronger than *ing-3(RNAi)* (Table 4). This confirmed our prediction that *ing-3* was involved in promoting germ cell apoptosis and validated our previous results based on RNAi. When *ing-3(RNAi)* was introduced into the *ing-3(tm2530)* mutant strain, the embryonic death rate and the number of apoptotic germ cells were the same as those of *ing-3(tm2530)* mutant (Table 4), suggesting that this *C. elegans ing-3* knockout strains was fully penetrant and the complete loss-of-function phenotypes have been obtained.

**Figure 16. IR-induced embryonic death rates**

IR-induced embryonic death rates of *ing-3(RNAi)* worms were higher than the wild-type, *unc-86(RNAi)* and *hda-6(RNAi)*, and comparable to that of *cep-1* worms. *cep-1(null); ing-3(RNAi)* strain did not show an enhanced phenotype than *cep-1* or *ing-3(RNAi)* strains.

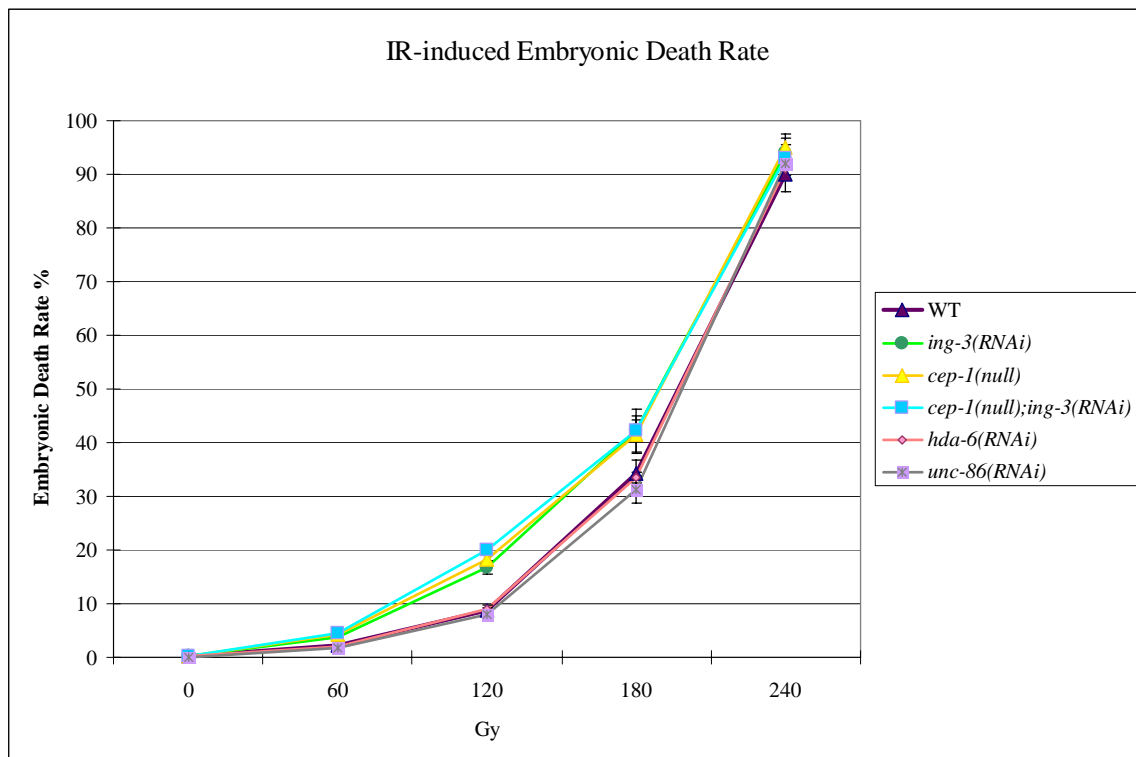


**Table 3. Embryonic death rates of different strains after 120Gy of IR**

n = total F1 counted (including dead eggs and hatched worms)

Genotype	Embryonic Death Rate (% , $\pm$ S.D.)
WT	9.4 ( $\pm$ 0.6) (n=3078)
<i>ing-3(RNAi)</i>	16.8 ( $\pm$ 1.3) (n=4266)
<i>ing-3(tm2530)</i>	22.7 ( $\pm$ 2.5) (n=3431)
<i>ing-3(ttTi5439)</i>	18.9 ( $\pm$ 2.1) (n=3340)
<i>ing-3(tm2530;RNAi)</i>	23.3 ( $\pm$ 4.3) (n=3125)
<i>cep-1</i>	18.2 ( $\pm$ 1.9) (n=3789)
<i>ing-3(RNAi); cep-1</i>	20.0 ( $\pm$ 1.7) (n=3672)
<i>hda-6(RNAi)</i>	9.6 ( $\pm$ 0.7 ) (n=2372)
<i>mcd-1(tm2169)</i>	10.2 ( $\pm$ 0.9) (n=2275)
<i>unc-86(RNAi)</i>	7.9 ( $\pm$ 0.8) (n=2283)

**Figure 17. IR-induced germ cell apoptosis**

L4 stage larvae were treated with 120 Gy of IR. Twenty-four hrs later, the number of apoptotic germ cells per gonad arm was counted. The apoptotic corpses possess flat round button-like morphology that can be recognized with Nomarski optics. In *ing-3(RNAi)* worms, there were fewer apoptotic germ cells (arrowhead) than in the wild-type worms.

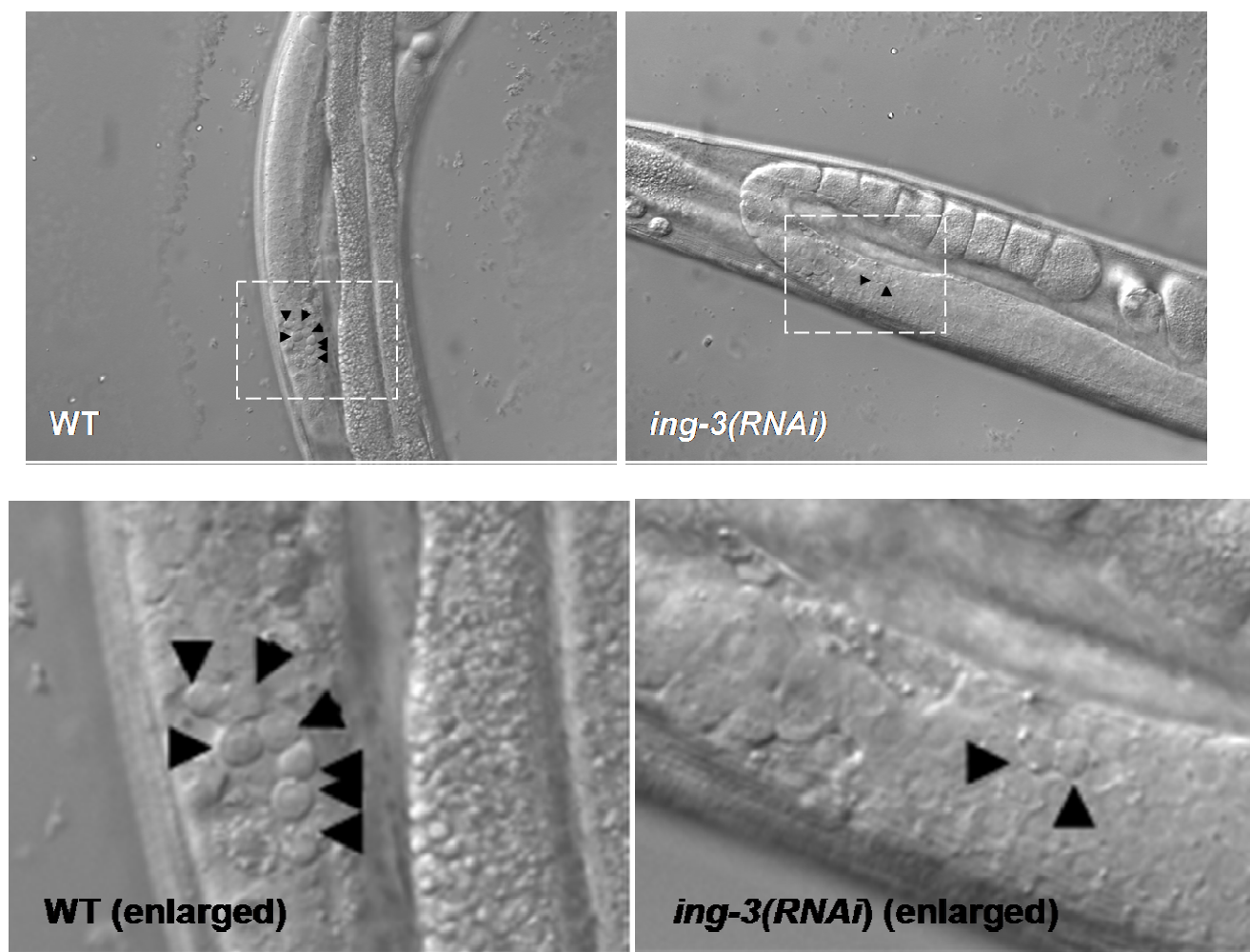


**Table 4. Number of germ cell corpses/gonad after 120Gy of IR**

n = total number of worms counted

<b>Genotype</b>	<b>Average germ cell corpses/per gonad arm (<math>\pm</math> S.D.)</b>
WT	13.5 ( $\pm$ 2.0) (n=40)
<i>ing-3(RNAi)</i>	6.3 ( $\pm$ 1.5) (n=40)
<i>cep-1(null)</i>	5.4 ( $\pm$ 0.8) (n=30)
<i>ing3(RNAi); cep-1(null)</i>	5.9 ( $\pm$ 1.2) (n=40)
<i>ing-3(tm2530)</i>	4.8 ( $\pm$ 1.2) (n=40)
<i>ing-3(tm2530; RNAi)</i>	4.9 ( $\pm$ 1.4) (n=30)
<i>ing-3(ttTi5439)</i>	6.7 ( $\pm$ 1.8) (n=45)

**Figure 18. ING-3 mutants**

In *ing-3(tm2530)*, the *ing-3* gene has a partial deletion in the 4<sup>th</sup> intron and the 5<sup>th</sup> exon, which might be translated into a 248 aa truncated protein with a predicted molecular mass of 27.9 kDa. In *ing-3(ttTi5439)* worms, the gene was interrupted by a Mos-1 insertion in the 4<sup>th</sup> exon and the first in-frame stop codon would result in a product of 17.2 kDa. Mouse polyclonal antibodies recognize a motif encoded by the 4<sup>th</sup> exon, which is upstream of both mutantions. Therefore the antibodies should be able to recognize these proteins encoded by the mutant genes if they are stable. Western blot results showed that the bands of 45kD in both knockout strains are missing and truncated proteins are not present, demonstrating that ING-3 proteins in these two strains are both completely depleted.

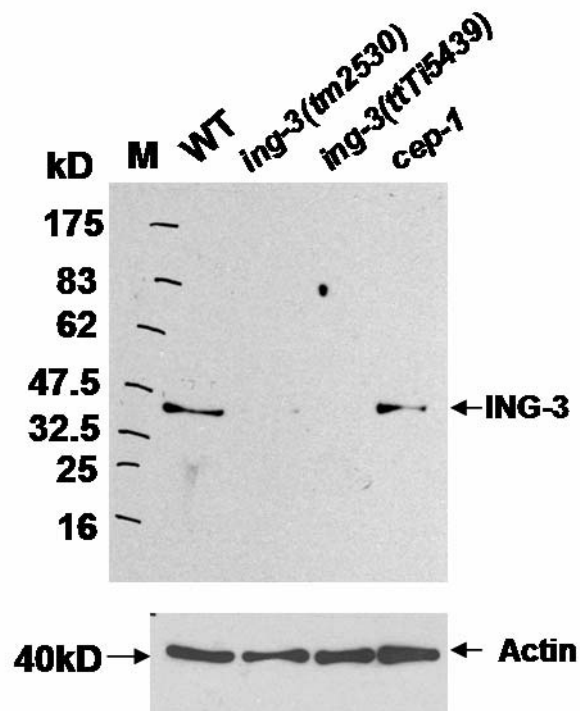
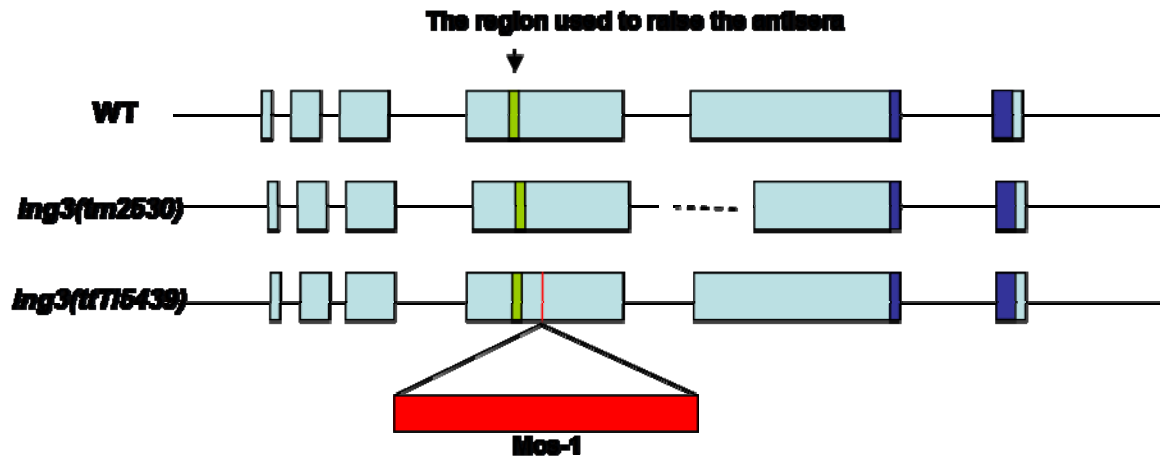
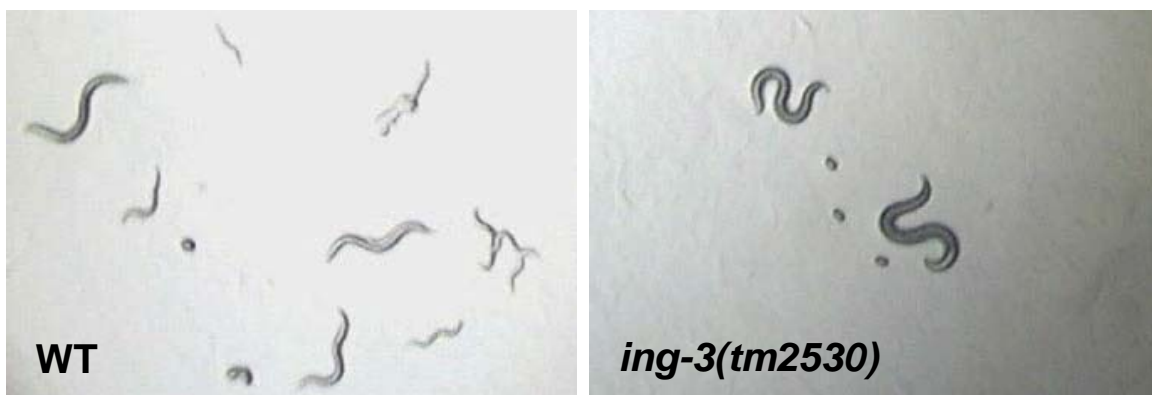


**Figure 19. The Unc phenotype of *ing-3* mutant strains**

Both of these *ing-3* mutant strains were viable but possessed a weak kinker uncoordinated phenotype. They bend with a sharper angle when moving and are slow in backing up after touching the head with a platinum wire.



## **CHAPTER IV: DISCUSSION**

### ***C. elegans ing-3* and IR-induced apoptosis**

In mammalian cells, both UV irradiation and ectopic overexpression of human ING3 proteins promote apoptosis, suggesting a role of human ING3 in mediating stress-induced apoptosis (Nagashima et al. 2003, Wang and Li, 2006). Consistent with this prediction, in *C. elegans*, IR-induced germ cell apoptosis is inhibited in both *ing-3(RNAi)* knockdown and *ing-3(null)* knockout worms. As a result, the embryonic death rate of the progeny of IR treated *ing-3* worms is higher than the wild-type control. Although the western blot showed that RNAi only reduced approximately half of the ING3 protein while in the knockout it was completely depleted, the embryonic death rate of the two mutant strains is only slightly higher than the RNAi worms. This result suggests that *C. elegans* is sensitive to relatively small changes in ING-3 expression.

Unlike gamma irradiation, depletion of ING-3 expression by RNAi did not elevate the embryonic death rate of F1 progeny following UV irradiation, indicating ING-3 does not function in UV-induced germ cell apoptosis. Likewise, preliminary results with heatshock treatment or oxidative stress by paraquat (methyl viologen dichloride hydrate, Sigma-Aldrich) (data not shown, one experiment each) showed that the *ing-3(RNAi)* worms did not show any difference in embryonic death rate. This result suggested that, in contrast to the mammalian homologs, the increased germ cell death mediated by *C. elegans* ING-3 is only induced by ionizing irradiation, but not affected by other stress.

When we plot the natural logarithm of the embryonic death rate of N2 and *ing-3* RNAi worms at various dosage of  $\gamma$ -irradiation, we found that there is a linear relationship (Figure 20). With the software Excel (Microsoft, USA), we got two linear

regression models for the IR-treated wide-type and *ing-3(RNAi)* strains:

$x$  = Dosage of IR (Gy),  $y$  = ln (Embryonic Death Rate)

WT:  $y = 60*(1.1422x - 4.6249)$ ,  $R^2 = 0.9969$

*ing-3(RNAi)*:  $y = 60*(0.9171x - 3.6744)$ ,  $R^2 = 0.997$

If Embryonic Death Rate = 50%,

Then  $y = -0.69315$

And  $x_{(WT)} = 206.5$  (Gy),  $x_{(ing3(RNAi))} = 195$  (Gy)

Therefore the median lethal dose ( $LD_{50}$ ) of the wide-type worms is 206.5 Gy while the  $LD_{50}$  of *ing-3(RNAi)* worms is a lower dosage of 195 Gy, which indicated that *ing-3(RNAi)* worms are hypersensitive to ionized irradiation. This result is consistent with a previous finding that ING1 knockout mice exhibited hypersensitivity to gamma irradiation (Kichina et al. 2006).

### **The roles of *ing-3* and *cep-1* in promoting stress-induced apoptosis**

Although dispensable for physiological germ cell death and developmental programmed cell death, *cep-1*, the *C. elegans* p53 homologue, has been shown to be required for DNA damage-induced apoptosis (Derry et al. 2001). In mammalian cells, ING proteins have been found to promote p53-dependent apoptosis. However, p53-independent apoptosis promoted by ING proteins has also been reported. Therefore the mechanism of ING apoptosis promotion needs to be clarified. Our data showed that the IR-induced apoptosis phenotype of *ing-3(RNAi)* worms is comparable to that of *cep-*

*l(null)* worms, so we suspect that these two genes function in the same apoptotic pathway in response to IR stress. Furthermore, since *ing-3(RNAi); cep-1(null)* resembles the phenotypes of *cep-1(null)* and *ing-3(RNAi)*, we concluded that *ing-3* and *cep-1* function in the same pathway.

To support this conclusion, ING-3 was overexpressed in wild type and *cep-1(null)* mutant backgrounds, then phenotypes were compared after IR. It was expected that an increase of *ing-3* would increase apoptosis in both backgrounds. However, probably due to the germline transgene silencing effect (Kelly and Fire 1998), although the western blot showed that ING-3 overexpression is induced after the heat shock treatment (which would detect both somatic and germline ING-3), the immunostaining showed that the ING-3 protein levels in gonad and embryos was not noticeably altered. Therefore, we could not test the effects of ING-3 overexpression.

Both CEP-1 and ING-3 protein are localized in the nucleus. However, their expression patterns in the adult hermaphrodite germlines only partially overlap. CEP-1 is expressed abundantly in mitotic germ cells in the distal arm, completely disappears from the transition zone and reappears in meiotic pachytene cells and remains during diakinesis stage (Schumacher et al. 2005). In our studies, we found that ING-3 is weakly expressed in mitotic germ cells but is strongly expressed in the transition zone and at the pachytene stage. The fact that they both localize in the pachytene nuclei, where apoptosis usually occurs, is consistent with our prediction that ING-3 and CEP-1/p53 function in the same pathway to promote IR-induced apoptosis. However, ING-3 is expressed in the transition zone while CEP-1 is not, suggesting that ING-3 and CEP-1 could be involved in distinct pathways/functions at different stages of germ line development.

### ***ing-3* and other genes**

In addition to *cep-1*, *hda-6* and *mcd-1* might also be functionally related to *ing-3* since they are in the same operon. Intriguingly, HDA-6 is a histone deacetylase (HDACs have been shown to interact with ING proteins) while MCD-1 is a C2H2-type zinc finger protein and recently has been found to regulate somatic cell apoptosis (Reddien et al. 2007). In a minority of cases, genes in the same *C. elegans* operon have been reported to regulate the same pathway. Therefore the role of *hda-6* and *mcd-1* in IR-induced germ cell apoptosis was investigated. *hda-6(RNAi)* and *mcd-1(tm2169)* was found to have no effect on IR-induced germline apoptosis and embryonic death rate, suggesting that *hda-6* and *mcd-1* are not involved in the IR-induced apoptosis pathway. However, this result does not exclude the possibility of their cooperation with ING-3 in other functions. Immunostaining results showed that in the nucleus, the pattern of ING-3 antibody staining and DAPI staining overlap. This could indicate that ING-3 can potentially interact with acetylation machinery and be involved in chromatin modification by acetylation or deacetylation in the nucleus as observed for other ING proteins in yeast and mammals. Therefore ING-3, HDA-6 and MCD-1 might function together in controlling chromatin modification.

*ing-1*, *ing-3*, *ing-4* triple RNAi was also tested by injection of dsRNA. These worms were viable and appeared normal without irradiation. When subjected to IR, they did not show any enhancement in the phenotypes compared to *ing-3 (RNAi)*. This result suggested that *ing-1* and *ing-4* are not redundant in regulating this IR-induced apoptosis pathway with *ing-3*.

Besides *ing-3* and *cep-1*, genes like *abl-1*, *clk-2*, *hus-1*, *mrt-2*, *ced-3*, *ced-9* and *egl-1* are all involved in DNA damage-induced *C. elegans* germ cell apoptosis (Deng et al. 2004). Therefore in the future we are interested in finding the genetic position of *ing-3* in the apoptotic pathway. The phenotypes of the strains depleted of *ing-3* and one of the above genes (represented by *gene A*) will be scored. If the double-mutant strain resembles the phenotype of *ing-3(null)* mutant strain, it will suggest that *ing-3* and *gene A* might function in the same pathway. If the double-mutant strain has a stronger phenotype than *ing-3* mutant strain, it will suggest that *gene A* might act either downstream of *ing-3* or function together with *ing-3* on a parallel pathway in the germ line. If the double mutant has a weaker phenotype than *ing-3* mutant alone, it will suggest that *gene A* might act either downstream of *ing-3* or functionally antagonize *ing-3* on a parallel pathway.

### **Tissue and cell-type specific functions of *ing-3***

*ing-3* is in an operon and appears to be transcribed from both the operon promoter and an internal promoter. *ing-3* promoter::GFP fusion experiments revealed different expression patterns of *ing-3* from each of its two promoters. The onset of zygotic *ing-3* gene expression is indicated by the reporter GFP expression, although the green fluorescence might be later than the genuine onset of endogenous *ing-3* gene expression. There is clearly a maternal contribution of the ING-3 protein before the onset of zygotic *ing-3* expression since we can see expression in the gonad and early embryos using ING-3 antibodies staining.

Although we could only document a function in the germline, it is interesting that

*ing-3* has two sets of promoters and they drive different expression patterns. The operon promoter drives ING-3 expression in many tissues including neurons, spermatheca, and vulva. The internal promoter drives ING-3 expression in both the anterior and the posterior ends of gut. For this internal specific promoter, ING-3 might be transcribed separately and independently with other genes in the same operon. In other tissues where ING-3 is driven by the operon promoter, ING-3 might function with other genes in the same operon, thus ING-3 function could vary in different tissues. Using this two-promoter-two-expression pattern, worms can easily vary ING-3 function in a tissue or time specific manner. In humans, ING3 has been found to have three splicing isoforms (<http://www.ncbi.nlm.nih.gov/>). Therefore, in a manner different from *C. elegans*, ING3 can take advantage of alternative splicing to alter function in different organs.

### **ING-3 in the intestine**

The intestine is one of the major organs of *C. elegans*, comprising about one third of the total somatic mass (McGhee et al. 2007). The *C. elegans* intestine is responsible for food digestion, absorption, energy metabolism, lipid storage, yolk synthesis, and probably the regulation of aging, lifespan, and stress response. It is a tube composed of a layer of only 20 epithelial cells. However, the cells differ in morphology, behaviour, nuclear divisions and gene expression patterns along the anterior-posterior axis. ING-3 is expressed mainly in the nuclei of the anteriormost intestine, suggested a possible role there. Since PHO-1 is an acid phosphatase expressed in all intestinal gut cells except the most anterior six cells (Fukushige et al. 2005), we tested whether *ing-3* inhibits *pho-1* expression in the anterior gut. *ing-3(RNAi)* was used on *pho-1::gfp* worms but there was

no change of GFP signal, suggesting *pho-1* is not downstream of *ing-3* (data not shown). The biological functions, the upstream regulators and the genes downstream of ING-3 in the intestine will be an interesting direction for further research.

### **ING-3 and chromatin regulation**

In both mammals and yeast, ING proteins interact with histone acetyltransferase or deacetylase complexes. However, prior to our work there was no previous evidence that endogenous ING proteins associate with chromatin *in vivo*. In the nucleus, the antibody staining of ING-3 precisely overlapped the DAPI pattern, suggesting that ING-3 might interact with the chromatin and perhaps function in chromatin regulation. The staining of ING-3 is not evenly distributed on chromatin, suggesting that ING-3 accumulates in specific regions. ING-3 might regulate chromatin structure by deacetylating or acetylating core histone proteins and influencing gene silencing or transcription. It will be intriguing to understand how ING-3 exerts epigenetic regulation in *C. elegans* and investigate whether HDA-6 and ING-3 are functionally related in future experiments.

### ***ing-3* and neural development/homeostasis**

Both *ing-3(tm2530)* and *ing-3(ttTi5439)* mutant strains possess a weak kinker Unc phenotype, showing defects in motility. In worms, body motility is controlled by both muscles and neurons. The kinker phenotype usually indicates a defect in neurons, implicating a role for ING3 in the regulation of neural development and/or function.

Although ING genes and proteins have evolved considerably in sequence during evolution, some functions such as pro-apoptotic regulation and chromatin modification

are well conserved. We were not surprised to find that the immunostaining of *C. elegans* ING-3 is overlapped with the DAPI staining of chromatin and *ing-3* is involved in promoting germ cell apoptosis in response to ionized irradiation. Here we propose that ING3 is evolutionally conserved in its neural function. We predicted that in humans, ING3 also possess a similar function and knockout of this gene might have consequences. It will be interesting to exploit the function of ING3 in mammalian systems for more information and wider scope to understand the biological functions of ING family proteins.

### **The importance of the *ing-3* gene**

*ing-3* RNAi and null mutations are viable, indicating that ING-3 is not essential for survival. However, this does not negate this protein's importance. Depletion of ING-3 did not affect physiological germline apoptosis but specifically reduced IR-induced apoptosis, suggesting that it responds to DNA double strand breaks caused by IR. This indicates the evolutionary conservation of the functions of ING3, since human ING3 has a role in mediating UV-induced apoptosis (Wang and Li, 2006). Ecotopic overexpression of human ING3 protein promoted apoptosis in a colon cancer cell line (Nagashima et al. 2003). We will test whether human ING3 can synergize with IR to promote apoptosis in cancer cells and further investigate the possibility of using ING3 to treat tumours in the clinical field. The location and expression level of human and *C. elegans* ING3 after IR treatment will also be studied to better understand the underlying mechanism.

**Conclusion and perspectives:**

The discovery that the role of ING3 in DNA damage-induced apoptosis is evolutionally conserved in *C. elegans* and human opens the way for the use of *C. elegans* genetics to uncover regulatory mechanisms and novel downstream targets of ING-3-mediated apoptosis. The fact that ING3 promoted DNA damage-induced apoptosis in the same pathway as CEP-1/p53 confirmed the close functional relationship between ING3 and p53 in mammalian systems. Since ING3 only affected DNA-damage-induced apoptosis but not physiological apoptosis, it also revealed a potential for therapeutic use of ING3.

**Figure 20. Linear relationship between the natural logarithm of the embryonic death rate and the dosage of  $\gamma$ -irradiation**

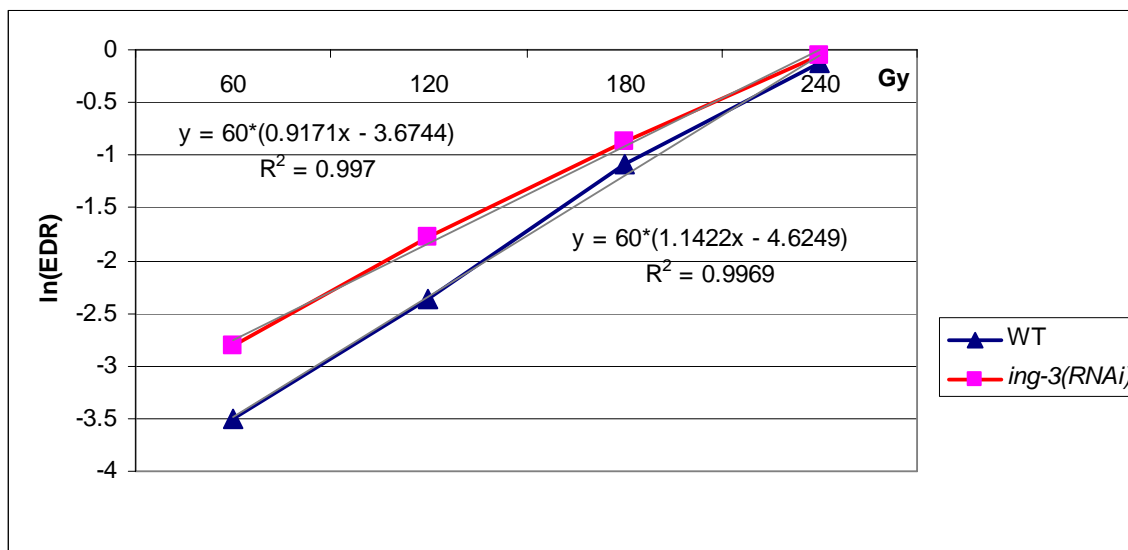
The natural logarithm of the embryonic death rate at 60, 120, 180 and 240 Gy of  $\gamma$ -irradiation were counted. There is a linear relationship between the natural logarithm of the embryonic death rate and the dosage of  $\gamma$ -irradiation in wild-type and *ing-3(RNAi)* worms.

The linear regression models are as following:

$$x = \text{Gy}, \quad y = \ln(\text{Embryonic Death Rate})$$

$$\text{WT:} \quad y = 60*(1.1422x - 4.6249), \quad R^2 = 0.9969$$

$$\text{ing-3 RNAi:} \quad y = 60*(0.9171x - 3.6744), \quad R^2 = 0.997$$



## REFERENCES

- Aballay A and Ausubel FM (2001) Programmed cell death mediated by *ced-3* and *ced-4* protects *Caenorhabditis elegans* from *Salmonella typhimurium*-mediated killing. *Proc. Natl. Acad. Sci. USA* 98, 2735–2739.
- Blumenthal T and Steward K. (1997) RNA Processing and Gene Structure. In *C. elegans II* (ed. D. L. Riddle, T. Blumenthal, B. J. Meyer and J. R. Priess), pp. 117-146. New York: Cold Spring Harbor Laboratory Press.
- Brenner, S. (1974) The Genetics of *Caenorhabditis elegans*. *Genetics* 77, 71–94.
- Chipuk JE, Kuwana T, Bouchier-Hayes L, Droin NM, Newmeyer DD, Schuler M et al. (2004). Direct activation of Bax by p53 mediates mitochondrial membrane permeabilization and apoptosis. *Science* 303: 1010–1014.
- Clark SG, Lu X, Horvitz HR (1994) The *Caenorhabditis elegans* locus *lin-15*, a negative regulator of a tyrosine kinase signaling pathway, encodes two different proteins. *Genetics* 137, 987-997.
- Coles AH, Liang H, Zhu Z, Marfella CG, Kang J, Imbalzano AN, Jones SN. (2007) Deletion of *p37<sup>Ing1</sup>* in mice reveals a p53-independent role for *Ing1* in the suppression of cell proliferation, apoptosis, and tumorigenesis. *Cancer Res.* 67, 2054-2061.
- Daniel NN, Korsmeyer SJ (2004) Cell death: critical control points. *Cell.* 116, 205-219. Review.
- Deng X, Hofmann ER, Villanueva A, Hobert O, Capodieci P, Veach DR, Yin X, Campodonico L, Glekas A, Cordon-Cardo C, Clarkson B, Bornmann WG, Fuks Z, Hengartner MO, Kolesnick R. (2004) *Caenorhabditis elegans* ABL-1 antagonizes p53-mediated germline apoptosis after ionizing irradiation. *Nat Genet.* 36, 906-912.

- Derry WB, Putzke AP, Rothman JH. (2001) *Caenorhabditis elegans* p53: role in apoptosis, meiosis, and stress resistance. *Science* 294, 591-595.
- Doyon Y, Selleck W, Lane WS, Tan S, Cote J. (2004) Structural and functional conservation of the NuA4 histone acetyltransferase complex from yeast to humans. *Mol Cell Biol.* 24, 1884-1896.
- Doyon Y, Cayrou C, Ullah M, Landry AJ, Cote V, Selleck W, Lane WS, Tan S, Yang XJ, Cote J. (2006) ING tumor suppressor proteins are critical regulators of chromatin acetylation required for genome expression and perpetuation. *Mol Cell.* 21, 51-64.
- Ellis HM, Horvitz HR. (1986) Genetic control of programmed cell death in the nematode *C. elegans*. *Cell* 44, 817-829.
- Feng X, Hara Y, Riabowol K. (2002) Different HATS of the ING1 gene family *Trends Cell Biol.* 12, 532-538. Review
- Feng, X., S. Bonni, and K. Riabowol, 2006 HSP70 induction by ING proteins sensitizes cells to tumor necrosis factor alpha receptor-mediated apoptosis. *Mol. Cell Biol.* 26: 9244-9255.
- Fisher DE (1994) Apoptosis in cancer therapy: Crossing the threshold. *Cell* 78, 539-542  
Review
- Fukushige T, Goszczynski B, Yan J, and McGhee JD. (2005) Transcriptional control and patterning of the *pho-1* gene, an essential acid phosphatase expressed in the *C. elegans* intestine. *Dev. Biol.* 279, 446-461.
- Garkavtsev I, Kazarov A, Gudkov A, Riabowol K. (1996) Suppression of the novel growth inhibitor p33ING1 promotes neoplastic transformation. *Nat Genet.* 14, 415-420
- Garkavtsev I, Kozin SV, Chernova O, Xu L, Winkler F, Brown E, Barnett GH, Jain RK.

- (2004) The candidate tumour suppressor protein ING4 regulates brain tumour growth and angiogenesis. *Nature* 18, 328-332
- Gartner A, Milstein S, Ahmed S, Hodgkin J and Hengartner MO. (2000) A conserved checkpoint pathway mediates DNA damage-induced apoptosis and cell cycle arrest in *C. elegans*. *Mol. Cell* 5, 435-443.
- Gartner A, MacQueen AJ and Villeneuve AM. (2004) Methods for analyzing checkpoint responses in *Caenorhabditis elegans*, *Methods Mol. Biol.* 280, 257-274.
- Gengyo-Ando, K., and Mitani, S. (2000) Characterization of mutations induced by ethyl methanesulfonate, UV, and trimethylpsoralen in the nematode *Caenorhabditis elegans*. *Biochem Biophys Res Commun* 269, 64-9
- Gong W, Suzuki K, Russell M, Riabowol K. (2005) Function of the ING family of PHD proteins in cancer. *Int J Biochem Cell Biol.* 37, 1054-1065. Review
- Gong W, Russell M, Suzuki K, Riabowol K. (2006) Subcellular targeting of p33ING1b by phosphorylation-dependent 14-3-3 binding regulates p21WAF1 expression. *Mol Cell Biol.* 26, 2947-2954.
- Gozani O, Karuman P, Jones DR, Ivanov D, Cha J, Lugovskoy AA, Baird CL, Zhu H, Field SJ, Lessnick SL, Villasenor J, Mehrotra B, Chen J, Rao VR, Brugge JS, Ferguson CG, Payrastre B, Myszka DG, Cantley LC, Wagner G, Divecha N, Prestwich GD, Yuan J. (2003) The PHD finger of the chromatin-associated protein ING2 functions as a nuclear phosphoinositide receptor. *Cell* 114, 99-111.
- Granger, L., Martin, E., and Segalat, L. (2004). Mos as a tool for genome-wide insertional mutagenesis in *Caenorhabditis elegans*: results of a pilot study. *Nucleic Acids Res* 32, e117

- Gumienny TL, Lambie E, Hartweg E, Horvitz HR, Hengartner MO. (1999) Genetic control of programmed cell death in the *Caenorhabditis elegans* hermaphrodite germline. *Development*. 126, 1011-1022.
- Ha S, Lee S, Chung M, Choi Y. (2002) Mouse ING1 homologue, a protein interacting with A1, enhances cell death and is inhibited by A1 in mammary epithelial cells. *Cancer Res*. 62, 1275-1278
- Hansen D, Hubbard EJ, Schedl T. (2004) Multi-pathway control of the proliferation versus meiotic development decision in the *Caenorhabditis elegans* germline. *Dev Biol*. 268, 342-357.
- He GH, Helbing CC, Wagner MJ, Sensen CW, Riabowol K. (2005) Phylogenetic analysis of the ING family of PHD finger proteins. *Mol Biol Evol*. 22, 104-116
- Helbing C, Veillette C, Riabowol K, Johnston RN, Garkavtsev I. (1997) A novel candidate tumor suppressor, ING1, is involved in the regulation of apoptosis. *Cancer Res*. 57, 1255-1258
- Hengartner MO. (1997) Cell Death. In *C. elegans II* (ed. D. L. Riddle, T. Blumenthal, B. J. Meyer and J. R. Priess), pp. 383-416. New York: Cold Spring Harbor Laboratory Press.
- Horn HF, Vousden KH. (2007) Coping with stress: multiple ways to activate p53. *Oncogene*. 26, 1306-1316. Review
- Horvitz HR, Brenner S, Hodgkin J, Herman RK. (1979) A uniform genetic nomenclature for the nematode *Caenorhabditis elegans*. *Mol Gen Genet*. 175, 129-133.
- Huang LS, Tzou P, Sternberg PW. (1994) The *lin-15* locus encodes two negative regulators of *Caenorhabditis elegans* vulval development. *Mol Biol Cell*. 5, 395-411.

- Hubbard EJ, Greenstein D. (2000) The *Caenorhabditis elegans* gonad: a test tube for cell and developmental biology. *Dev Dyn.* 218, 2-22.
- Joerger AC and Fersht AR. (2007) Structure–function–rescue: the diverse nature of common p53 cancer mutants. *Oncogene* 26, 2226–2242. Review
- Kelly WG, Fire A. (1998) Chromatin silencing and the maintenance of a functional germline in *Caenorhabditis elegans*. *Development.* 125, 2451-2456.
- Kichina JV, Zeremski M, Aris L, Gurova KV, Walker E, Franks R, Nikitin AY, Kiyokawa H, Gudkov AV. (2006) Targeted disruption of the mouse *ing1* locus results in reduced body size, hypersensitivity to radiation and elevated incidence of lymphomas. *Oncogene* 25, 857–866
- Kuzmichev A, Zhang Y, Erdjument-Bromage H, Tempst P, Reinberg D. (2002) Role of the Sin3-histone deacetylase complex in growth regulation by the candidate tumor suppressor p33(ING1). *Mol Cell Biol.* 22, 835-848.
- Lette G, Kritikou EA, Jaeggi M, Calixto A, Fraser AG, Kamath RS, Ahringer J, Hengartner MO. (2004) Genome-wide RNAi identifies p53-dependent and -independent regulators of germ cell apoptosis in *C. elegans*. *Cell Death Differ.* 11, 1198-1203.
- Loewith R, Meijer M, Lees-Miller SP, Riabowol K, Young D. (2000) Three yeast proteins related to the human candidate tumor suppressor p33(ING1) are associated with histone acetyltransferase activities. *Mol Cell Biol.* 20, 3807-3816.
- Lu F, Dai DL, Martinka M, Ho V, Li G. (2006) Nuclear ING2 expression is reduced in human cutaneous melanomas. *Br J Cancer.* 95, 80-86.
- Mayanagi T, Amagai A, Maeda Y. (2005) DNG1, a *Dictyostelium* homologue of tumor suppressor ING1 regulates differentiation of *Dictyostelium* cells. *Cell Mol Life Sci.*

62, 1734-1743.

McGhee JD, Sleumer MC, Bilenky M, Wong K, McKay SJ, Goszczynski B, Tian H, Krich ND, Khattrra J, Holt RA, Baillie DL, Kohara Y, Marra MA, Jones SJ, Moerman DG, Robertson AG. (2007) The ELT-2 GATA-factor and the global regulation of transcription in the *C. elegans* intestine. *Dev Biol.* 302, 627-645.

Mello C (1991)

Mello C and Fire A (1995). DNA transformation. In *Caenorhabditis elegans: Modern Biological Analysis of an Organism*, Vol. 48 (ed. D. Shakes and H. Epstein), pp. 451-482. London: Academic Press.

Mihara M, Erster S, Zaika A, Petrenko O, Chittenden T, Pancoska P and Moll UM. (2003) p53 has a direct apoptogenic role at the mitochondria. *Mol. Cell* 11, 577-590.

Miller DM, Shakes DC. (1995) Immunofluorescence microscopy. In Epstein H.F., Shakes D.C., eds. *Caenorhabditis elegans: Modern Biological Analysis of an Organism*. San Diego, CA, Academic Press, Inc., 365-394.

Nagashima G, Shiseki M, Miura K, Hagiwara K, Linke SP, Pedoux R, Wang XW, Yokota J, Riabowol K, Harris CC. (2001) DNA damage-inducible gene p33ING2 negatively regulates cell proliferation through acetylation of p53. *Proc Natl Acad Sci U S A.* 98, 9671-9676.

Nagashima G, Shiseki M, Pedoux RM, Okamura S, Kitahama-Shiseki M, Miura K, Yokota J, Harris CC. (2003) A novel PHD-finger motif protein, p47ING3, modulates p53-mediated transcription, cell cycle control, and apoptosis. *Oncogene.* 22, 343-350.

Nouman GS, Anderson JJ, Crosier S, Shrimankar J, Lunec J, Angus B. (2003) Downregulation of nuclear expression of the p33(ING1b) inhibitor of growth protein

- in invasive carcinoma of the breast. *J. Clin. Pathol.* 56, 507-511
- Nourani A, Howe L, Pray-Grant MG, Workman JL, Grant PA, Cote J. (2003) Opposite role of yeast ING family members in p53-dependent transcriptional activation. *J Biol Chem.* 278, 19171-19175.
- Peña PV, Davrazou F, Shi X, Walter KL, Verkhusha VV, Gozani O, Zhao R, Kutateladze TG (2006) Molecular mechanism of histone H3K4me3 recognition by plant homeodomain of ING2 *Nature* 442, 100-103
- Pedoux R, Sengupta S, Shen JC, Demidov ON, Saito S, Onogi H, Kumamoto K, Wincovitch S, Garfield SH, McMenamin M, Nagashima M, Grossman SR, Appella E, Harris CC. (2005) ING2 regulates the onset of replicative senescence by induction of p300-dependent p53 acetylation. *Mol Cell Biol.* 25, 6639-6648.
- Reddien PW, Andersen EC, Huang MC, Horvitz HR. (2007) DPL-1 DP, LIN-35 Rb and EFL-1 E2F Act With the MCD-1 Zinc-Finger Protein to Promote Programmed Cell Death in *Caenorhabditis elegans*. *Genetics.* 175, 1719-1733.
- Riddle DL and Albert PS. (1997). Genetic and Environmental Regulation of Dauer Larva Development. In *C. elegans II* (ed. D. L. Riddle, T. Blumenthal, B. J. Meyer and J. R. Priess), pp. 739-768. New York: Cold Spring Harbor Laboratory Press.
- Riddle DL, Blumenthal T, Meyer BJ and Priess JR. (1997). Introduction to *C. elegans*. In *C. elegans II* (ed. D. L. Riddle, T. Blumenthal, B. J. Meyer and J. R. Priess), pp. 1-22. New York: Cold Spring Harbor Laboratory Press.
- Russell M, Berardi P, Gong W, Riabowol K. (2006) Grow-ING, Age-ING and Die-ING: ING proteins link cancer, senescence and apoptosis. *Exp Cell Res.* 312, 951-961.
- Salinas LS, Maldonado E, Navarro RE. (2006) Stress-induced germ cell apoptosis by a p53

- independent pathway in *Caenorhabditis elegans*. *Cell death differ.* 13, 2129-2139.
- Sambrook J, Fritsch EF, Maniatis T. (1989) *Molecular Cloning*, New York: Cold Spring Harbor Laboratory Press.
- Schedl T. (1997) Developmental Genetics of the Germ Line. In *C. elegans II* (ed. D. L. Riddle, T. Blumenthal, B. J. Meyer and J. R. Priess), pp. 241-270. New York: Cold Spring Harbor Laboratory Press.
- Schumacher B, Hofmann K, Boulton S, Gartner A. (2001) The *C. elegans* homolog of the p53 tumor suppressor is required for DNA damage-induced apoptosis. *Curr Biol.* 11, 1722-1727.
- Schumacher B, Schertel C, Wittenburg N, Tuck S, Mitani S, Gartner A, Conradt B, Shaham S. (2005) Translational repression of *C. elegans* p53 by GLD-1 regulates DNA damage-induced apoptosis. *Cell.* 120, 357-368.
- Scott M, Boisvert FM, Vieyra D, Johnston RN, Bazett-Jones DP, Riabowol K. (2001) UV irradiation induces nucleolar translocation of ING1 through two distinct nucleolar targeting sequences. *Nucleic Acids Res.* 29, 2052–2058.
- Shi X, Hong T, Walter KL, Ewalt M, Michishita E, Hung T, Carney D, Pena P, Lan F, Kaadige MR, Lacoste N, Cayrou C, Davrazou F, Saha A, Cairns BR, Ayer DE, Kutateladze TG, Shi Y, Cote J, Chua KF, Gozani O. (2006) ING2 PHD domain links histone H3 lysine 4 methylation to active gene repression. *Nature* 442, 96-99.
- Shinoura N, Muramatsu Y, Nishimura M, Yoshida Y, Saito A, Yokoyama T, Furukawa T, Horii A, Hashimoto M, Asai A, Kirino T, Hamada H. (1999) Adenovirus-mediated transfer of p33ING1 with p53 drastically augments apoptosis in gliomas. *Cancer Res.* 59, 5521–5528

- Shiseki M, Nagashima M, Pedoux RM, Kitahama-Shiseki M, Miura K, Okamura S, Onogi H, Higashimoto Y, Appella E, Yokota J, Harris CC. (2003) p29ING4 and p28ING5 bind to p53 and p300, and enhance p53 activity. *Cancer Res.* 63, 2373-2378.
- Stergiou L, Doukoumetzidis K, Sendoel A, Hengartner MO. (2007) The nucleotide excision repair pathway is required for UV-C-induced apoptosis in *Caenorhabditis elegans*. *Cell Death Differ.* 14, 1129-1138.
- Sulston JE, Horvitz HR. (1977) Post-embryonic cell lineages of the nematode, *C. elegans*. *Dev Biol.* 56, 110-156.
- Takanami T, Mori A, Takahashi H, Higashitani A. (2000) Hyper-resistance of meiotic cells to radiation due to a strong expression of a single recA-like gene in *Caenorhabditis elegans*. *Nucleic Acids Res.* 28, 4232-4236.
- Timmons L and Fire A. (1998) Specific interference by ingested dsRNA. *Nature*, 395, 854.
- Timmons L. (2001) Ingestion of bacterially expressed dsRNAs can produce specific and potent genetic interference in *Caenorhabditis elegans*. *Gene.* 263, 103-112
- Treinin M, Gillo B, Liebman L, Chalfie M. (1998) Two functionally dependent acetylcholine subunits are encoded in a single *Caenorhabditis elegans* operon. *Proc Natl Acad Sci U S A.* 95, 15492–15495.
- Tsang FC, Po LS, Leung KM, Lau A, Siu WY, Poon RY. (2003) ING1b decreases cell proliferation through p53-dependent and -independent mechanisms. *FEBS Lett.* 553, 277-285.
- Vieyra D, Toyama T, Hara Y, Boland D, Johnston R, Riabowol K. (2002) ING1 isoforms differentially affect apoptosis in a cell age-dependent manner. *Cancer Res.* 62, 4445-4452

- Vieyra, D, Senger DL, Toyama T, Muzik H, Brasher PM, Johnston RN, Riabowol K, Forsyth PA. (2003) Altered subcellular localization and low frequency of mutations of ING1 in human brain tumors. *Clin. Cancer Res.* **9**, 5952-5961
- Wagner MJ, Gogela-Spehar M, Skirrow RC, Johnston RN, Riabowol K, Helbing CC. (2001) Expression of novel ING variants is regulated by thyroid hormone in the *Xenopus laevis* tadpole. *J Biol Chem.* 276, 47013-47020.
- Wang Y, Li G. (2006) ING3 promotes UV-induced apoptosis via fas/caspase-8 pathway in melanoma cells. *J Biol Chem* 281, 11887-11893.
- Wang Y, Wang J, Li G. (2006) Leucine zipper-like domain is required for tumor suppressor ING2-mediated nucleotide excision repair and apoptosis. *FEBS Lett.* 580, 3787-3793.
- Zdinak LA, Greenberg IB, Szewczyk NJ, Barmada SJ, Cardamone-Rayner M, Hartman JJ, Jacobson LA. (1997) Transgene-coded chimeric proteins as reporters of intracellular proteolysis: Starvation-induced catabolism of a lacZ fusion protein in muscle cells of *Caenorhabditis elegans*. *J. Cell. Biochem.* **67**: 143-153.
- Zhu JJ, Li FB, Zhou JM, Liu ZC, Zhu XF, Liao WM. (2005) The tumor suppressor p33ING1b enhances taxol-induced apoptosis by p53-dependent pathway in human osteosarcoma U2OS cells. *Cancer Biol Ther.* 4, 39-47.

**APPENDIX****β-gal staining solution**

20 μl 2.5% X-Gal

100 μl Redox buffer (5 mM K. Ferrocyanide, 5 mM K. Ferricyanide)

400 μl 1 M sodium phosphate buffer (pH 7.5)

2 μl 1 M MgCl<sub>2</sub>

4 μl 1% SDS

470 μl water

**Blocking solution for western blot**

PBST

10% non-fat milk powder

**Commassie staining solution**

1.0% (W/V) Coomassie brilliant blue R-250 (Biorad)

10% (V/V) methanol

15% (V/V) glacial acetic acid

complete the volume with distilled water

**6X DNA loading buffer**

0.25% (W/V) bromophenol blue

0.25% (W/V) xylene cyanol FF

30% glycerol

**Destained solution**

10% (V/V) methanol

15% (V/V) glacial acetic acid

0.5% (V/V) glycerol

complete the volume with distilled water

**3% formaldehyde/0.1M KPO<sub>4</sub> (PH 7.2)**

3.73 mL 1M K<sub>2</sub>HPO<sub>4</sub>

1.47 mL 1M KH<sub>2</sub>PO<sub>4</sub>

10 mL 16% formaldehyde

36.8 mL ddH<sub>2</sub>O

**2X Laemmli sample buffer**

100 mM Tris PH 6.8

200 mM dithiothreitol (DTT)

4% SDS

0.2% bromophenol blue

20% glycerol

**LB broth**

10 g of tryptone

5 g of yeast extract

10 g of NaCl

complete the volume with distilled water

**M9**

6 g of Na<sub>2</sub>HPO<sub>4</sub>

3 g of KH<sub>2</sub>PO<sub>4</sub>

5 g of NaCl

0.25 g of MgSO<sub>4</sub>·7H<sub>2</sub>O

complete the volume to a total of 1L with distilled water

### **PBS**

8 g NaCl

0.2 g KCl

1.44 g Na<sub>2</sub>HPO<sub>4</sub>

0.24 g KH<sub>2</sub>PO<sub>4</sub>

H<sub>2</sub>O to 1 L, then adjust PH to 7.4

### **PBST**

PBS buffer

0.5% (V/V Tween 20)

### **Resolving gel for SDS-PAGE**

10 to 15% acrylamide:bisacrylamide (29:1 ratio)

380 mM Tris PH 8.8

0.1% SDS

0.5% mg/mL ammonium persulfate (APS)

0.05% (V/V) N,N,N',N'-tetramethylethyldiamine (TEMED)

### **Running buffer for SDS-PAGE**

25mM Tris PH 8.5

0.2M glycine

5% (V/V) glycerol

0.1% SDS

### **Stacking gel for SDS-PAGE**

5% acrylamide (W/W)

0.09% bisacrylamide (W/W)

0.1% SDS

145 mM Tris PH 6.8

1 mg/mL APS

0.05% (V/V) TEMED

### **50X TAE**

242g of Tris base

57mL glacial acetic acid

100mL of 0.5M EDTA PH 8.0

complete the volume to a total of 1L with distilled water

### **Transfer buffer**

800mL of distilled water

3g of Tris-Base

14.4 g of glycine

200mL of methanol

### **Worm lysis buffer**

50 mM KCl

10 mM Tris pH 8.3

2.5 mM MgCl<sub>2</sub>

0.45% NP-40 (IGEPAL)

0.45% Tween-20

0.01% Gelatin